


 Cite this: *Lab Chip*, 2026, 26, 1489

## AI-enabled wearable microfluidics for next-generation infection monitoring and therapeutics

 Yan Zhou,<sup>ab</sup> Xiaoyu Zhu,<sup>ab</sup> Kai Qu<sup>\*cd</sup> and Feng Xu <sup>\*ab</sup>

Wearable biosensors have revolutionized healthcare by enabling continuous, minimally invasive monitoring of health parameters. While traditional wearables primarily measure physiological signals, recent advancements now allow biochemical sensing of microbial biomarkers across diverse human biofluids, including sweat, saliva, wound exudate, interstitial fluid, tears, breath, and urine. These biomarkers, including microbial nucleic acids, metabolites, and host immune mediators, provide valuable information for diagnosing and managing infections. Wearable microfluidic devices are designed to sample these biofluids directly from the body and allow for rapid identification of microbial signatures and associated host responses. Moreover, some wearables' use of living microorganisms as functional components has opened new opportunities for biosensing and therapeutic delivery. The integration of artificial intelligence improves the interpretation of complex and dynamic data streams, and facilitates precise and adaptive decision-making. Additionally, by addressing biomechanical interactions between microorganisms, host tissues, and wearable interfaces, mechanomedicine principles provide insights into these systems. In the near future, these interdisciplinary innovations have the potential to transform infection control, personalized healthcare, and global health surveillance.

 Received 24th July 2025,  
 Accepted 26th October 2025

DOI: 10.1039/d5lc00733j

[rsc.li/loc](https://rsc.li/loc)

### 1. Introduction

Wearable devices have transformed healthcare by enabling continuous, decentralized, and minimally invasive monitoring of physiological and biochemical health indicators.<sup>1,2</sup> Commercial wearable devices like smartwatches and fitness trackers are primarily focused on physical parameters like heart rate and electrocardiogram (ECG).<sup>3</sup> Recent advances in microfluidics and bioengineering have further enhanced these systems to biochemical sensing across various human biofluids, such as sweat, saliva, wound exudate, interstitial fluid (ISF), urine, exhaled breath condensate (EBC), and tears.<sup>4–6</sup> These fluids contain critical biomarkers reflective of health conditions, particularly infectious diseases, where timely detection and monitoring are crucial for effective management.

Microorganisms, whether commensal, pathogenic, or probiotic, significantly influence human health and disease states. The ability to detect microbial biomarkers, such as DNA/RNA, toxins, and metabolites, as well as host immune responses, at the point of care offers potential for personalized medicine. Each biofluid uniquely mirrors different aspects of infection. Saliva and EBC, for instance, are ideal for identifying respiratory infections, whereas wound fluid contains immune responses and local microbial toxins. Because of its dynamic compositions, host-derived interference, and low analyte concentrations, each biofluid poses analytical challenges. Integrated microfluidic systems for multi-fluid sampling and real-time analysis are necessary to overcome these constraints.

Innovations in microfluidic design now allow for real-time sampling and analysis through compact devices such as skin-conformal patches, microneedles, contact lenses, masks, and catheter-based sensors. These systems not only enable continuous sampling and detection of microbial signatures, but also integrate engineered microorganisms as functional biosensing components.<sup>7–9</sup> Such biosystem-integrated devices further advance microbial metabolism for specific biomarker detection, energy harvesting, and responsive therapeutic delivery. These new developments mark a big change toward biologically intelligent wearable devices that work closely with the body, opening up new ways to monitor health and provide treatment.

<sup>a</sup> The Key Laboratory of Biomedical Information Engineering of Ministry of Education, School of Life Science and Technology, Xi'an Jiaotong University, Xi'an 710049, Shaanxi, P.R. China. E-mail: fengxu@mail.xjtu.edu.cn

<sup>b</sup> Bioinspired Engineering and Biomechanics Center (BEBC), Xi'an Jiaotong University, Xi'an 710049, Shaanxi, P.R. China

<sup>c</sup> Department of Hepatobiliary Surgery and Liver Transplantation, The Second Affiliated Hospital of Xi'an Jiaotong University, Xi'an 710004, P.R. China. E-mail: qukai001@xjtu.edu.cn

<sup>d</sup> Key Laboratory of Surgical Critical Care and Life Support (Xi'an Jiaotong University), Ministry of Education, P.R. China



Fig. 1 A representative system of AI-enabled wearable microfluidics for next generation infection monitoring and therapies.

The integration of artificial intelligence (AI) further enhances the capabilities of these wearable microfluidic systems. Machine learning and deep learning algorithms help enhance analytical accuracy by interpreting complex sensor signals, distinguishing subtle infection-related patterns from physiological noise,<sup>10</sup> and enabling accurate, predictive analytics.<sup>9</sup> For example, deep

learning models can correlate cytokine levels with physiological parameters or distinguish bacterial from viral infection profiles based on biomarker profiles.<sup>11</sup> In addition, mechanical factors such as fluid shear stress, skin deformation, and biofilm mechanics are increasingly recognized as integral parameters of microbial behavior and sensor performance.<sup>12,13</sup> AI-driven analytics can help analyze these mechanical forces that significantly influence host-microbe interactions, optimizing sensor performance and therapeutic efficacy. Integration with Internet of Things (IoT) technology further enhances communication with healthcare providers and supports closed-loop feedback systems for infection management.<sup>14</sup>

This review takes an integrated perspective on AI-enabled wearable microfluidics focused on microbial biomarkers and living microorganisms as sensing and therapeutic elements (Fig. 1). We highlight developments combining microbial biosensors and AI-driven analytics, talk about breakthroughs in a variety of biofluids, and emphasize the mechanomedical aspects that support system performance. Finally, we discuss current issues and future perspectives, envisioning a new generation of biologically integrated, intelligent wearable systems that can provide individualized healthcare interventions and infectious disease monitoring.

## Tear

*S. aureus*, *P. aeruginosa*  
*S. pneumoniae*  
*M. morgani*

## Saliva

*S. salivarius*, *P. gingivalis*  
*H. pylori*, *S. mutans*  
SARS-CoV-2

## Wound exudate

*S. aureus*  
*P. aeruginosa*  
*E. coli*

## EBC

*M. tuberculosis*  
SARS-CoV2  
Rhinoviruses  
Influenza

## ISF

*P. falciparum*, *S. aureus*  
*P. aeruginosa*, *C. tetani*  
SARS-CoV-2

## Urine

*E. coli*

## Sweat

*S. aureus*, *C. acnes*  
Proteobacteria  
Actinobacteria  
Bacteroidetes

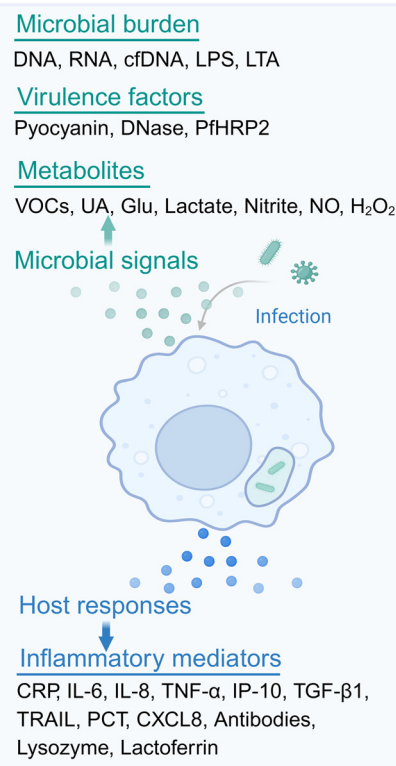


Fig. 2 Schematic overview of pathogens across human biofluids including tears, saliva, wound fluid, exhaled breath condensate (EBC), interstitial fluid (ISF), sweat, and urine, along with associated wearable devices such as lenses, patches, masks, microneedles, bandages, and catheter bags. The right panel summarizes categories of microbial signals and host responses during infection.

## 2. Wearable microfluidics for microbial sensing

The efficacy of conventional laboratory-based infection diagnostics in timely decision-making is often limited by invasive sampling and time-consuming procedures. Wearable microfluidic systems represent an advancement in healthcare that enables rapid and noninvasive monitoring of microbial infections through real-time analysis of body fluids (Fig. 2). Peripheral biofluids, such as wound exudate, sweat, ISF, saliva, tears, and urine, contain appreciable concentrations of biomarkers valuable for infection diagnosis (Table 1). To continuously monitor at the point of care, these platforms combine electrochemical, optical, and molecular sensing techniques with integrated microfluidic designs (Table 2).

### 2.1 Dermal fluid-based infection diagnostics

Sweat, ISF, and wound exudate are examples of dermal biofluids that offer easily accessible biomarkers that represent both localized and systemic infections. For example, eccrine sweat is perfect for noninvasive immune surveillance, since it contains inflammatory cytokines,<sup>15</sup> chemokines,<sup>16,17</sup> and acute-phase proteins<sup>18</sup> mirroring blood

concentrations during infections (Table 1). The SWEATSENDER device demonstrated the feasibility of tracking cytokines and other proteins such as IL-6, IL-8, IL-10, TNF- $\alpha$ , IP-10, TRAIL, and CRP in passive sweat (Fig. 3a and b), distinguishing individuals with flu-like illness (Table 2).<sup>15,19,20</sup> The Sweat AWARE platform that monitored TNF- $\alpha$ , IL-6, and CRP showed a strong correlation between sweat and serum levels in infection cases (Fig. 3c and d).<sup>21</sup> Similarly, the InflaStat microfluidic patch incorporates immunoassays to provide reliable sweat-based inflammation profiling with real-time calibration, demonstrating clinical feasibility for continuous, decentralized monitoring (Fig. 3e).<sup>22</sup>

ISF, accessed minimally invasively *via* microneedles, closely mirrors plasma composition.<sup>23,24</sup> It contains infection-related biomarkers such as inflammatory cytokines,<sup>25,26</sup> host and pathogen-derived cell-free DNA,<sup>27–30</sup> and pathogen-specific antigens and antibodies.<sup>31–33</sup> Innovative microneedle platforms were employed for molecular diagnostics. For example, a hollow microneedle patch that integrated a lateral flow immunoassay (LFA) for detecting *Pf*HRP2 achieved malaria diagnosis from ISF.<sup>34</sup> A related 3D-printed patch enabled dual detection of CRP and procalcitonin (PCT) for bacterial infection and sepsis (Table 2).<sup>35</sup> Advanced platforms incorporating a CRISPR-Cas9 sensor detected cfDNA of Epstein–Barr virus and

**Table 1** Major biomarkers in each type of body fluid and the associated pathogens

| Type of body fluid                              | Biomarker  | Target bacteria  | Ref.                                    |             |
|---|--|--|---|-------------|
| Sweat   | DNA, RNA   | <i>Proteobacteria</i> , <i>Actinobacteria</i> , <i>Bacteroidetes</i>                       | 174                                     |             |
|   | IP-10, TRAIL, CRP                                | <i>S. aureus</i> , <i>C. acnes</i>   | 18, 175                                 |             |
| ISF   | cfDNA  | Pathogen infection   | 25                                      |             |
|   | Pyocyanin  | <i>P. aeruginosa</i>   | 30                                      |             |
|   | PfHRP2   | <i>Plasmodium falciparum</i>   | 31                                      |             |
|   | TNF- $\alpha$ , IL-1 $\beta$ , IL-6              | <i>S. aureus</i> , <i>P. aeruginosa</i>  | 27                                      |             |
|   | Anti-tetanus toxoid IgG                          | <i>Clostridium tetani</i>  | 32                                      |             |
|   | SARS-CoV-2 antibodies                            | SARS-CoV-2   | 33                                      |             |
|   | Uric acid, lactate, glucose                      | <i>S. aureus</i> , <i>C. violaceum</i> , <i>P. aeruginosa</i>                              | 29, 176                                 |             |
|   | pH   | Bacterial infection  | 28                                      |             |
|   | Wound fluid                                      | DNA/RNA  | <i>S. aureus</i>                        | 67          |
|   |  | Pyocyanin, DNase   | <i>P. aeruginosa</i> , <i>S. aureus</i> | 38, 46, 177 |
| TGF- $\beta$ 1, TNF- $\alpha$ , IL-6, IL-8, CRP |  | <i>S. aureus</i> , <i>P. aeruginosa</i> , <i>E. coli</i>                                   | 47–53                                   |             |
| Uric acid, lactate, glucose, TMA                |  | <i>S. aureus</i> , <i>P. aeruginosa</i> , <i>E. coli</i>                                   | 39–41, 54, 55, 178                      |             |
| Temperature, pH                                 |  | <i>S. aureus</i> , <i>E. coli</i>  | 56, 57                                  |             |
| NO  |  | <i>P. aeruginosa</i>   | 59, 179                                 |             |
| H <sub>2</sub> O <sub>2</sub>                   |  | <i>S. aureus</i> , <i>P. aeruginosa</i>  | 180                                     |             |
| Saliva  |  | DNA, RNA, LPS, LTA   | <i>S. salivarius</i>                    | 73          |
|   | IL-1 $\beta$ , IL-6, MMPs                        | <i>S. mutans</i> , <i>P. gingivalis</i> , <i>Haemophilus</i>                               | 77, 181                                 |             |
|   | sIgA   | SARS-CoV-2   | 78, 80                                  |             |
|   | pH, lactate                                      | <i>S. mutans</i>   | 82                                      |             |
| Tears   | DNA, RNA, LPS                                    | <i>P. aeruginosa</i>   | 87                                      |             |
|   | Lysozyme, lactoferrin                            | Bacterial infection  | 88                                      |             |
|   | IL-1 $\beta$ , IL-6, TNF- $\alpha$ , IL-8, CXCL8 | <i>S. aureus</i> , <i>S. pneumoniae</i> , <i>P. aeruginosa</i> , <i>M. morgani</i>         | 90                                      |             |
|   | Glucose, nitrite, pH                             | <i>S. epidermidis</i> , <i>S. viridans</i>   | 91                                      |             |
| EBC   | DNA, RNA   | <i>M. tuberculosis</i>   | 96                                      |             |
|   | Specific antibodies                              | Rhinoviruses, enteroviruses  | 182                                     |             |
|   | PCT, CRP   | <i>Klebsiella</i> , <i>streptococcus</i> ,<br><i>Influenza A virus</i> , <i>Adenovirus</i> | 97                                      |             |
|   | VOCs   | SARS-CoV-2   | 93                                      |             |
| Urine   | DNA, RNA   | <i>E. coli</i>   | 106                                     |             |
|   | PCT, CRP   |  | 109, 110                                |             |
|   | <i>E. coli</i> -specific enzymes                 |  | 183                                     |             |
|   | Nitrite  |  | 102                                     |             |

Table 2 Wearable microfluidics for detection of infectious disease-related microorganisms

| Biofluids   | Biomarker  | Microorganism                             | Platform                       | Recognition element  | Mechanism   | Linear range (LOD)  | Ref. |
|-------------|--|---|--------------------------------|--|---|---|------|
| Sweat       | IP-10, TRAIL                                     | Infection                                 | Wearable patches               | Capture probe antibody   | EIS   | IP-10 & TRAIL: 1–512 pg mL <sup>-1</sup><br>(1 pg mL <sup>-1</sup> )  | 20   |
|             | CRP  |   |                                |  |   | CRP: 0.2–204 ng mL <sup>-1</sup><br>(0.2 ng mL <sup>-1</sup> )  |      |
| ISF         | CRP  | Infection                                 | Sweat patch                    | cAbs and dAb-immobilized AuNPs   | SWV   | CRP: 0–20 ng mL <sup>-1</sup> (8 pM)  | 22   |
|             | <i>Pf</i> HRP2                                   | <i>Plasmodium falciparum</i>              | Microneedle patch              | Anti- <i>Pf</i> HRP2 IgM& IgG antibodies   | Colorimetric  | <i>Pf</i> HRP2: 0–1024 ng mL <sup>-1</sup><br>(8 ng mL <sup>-1</sup> )  | 34   |
|             | CRP, PCT   | Infection                                 | Microneedle patch              | LFA antibody   | Colorimetric/fluorescence   | CRP: 0–500 µg mL <sup>-1</sup><br>(10 µg mL <sup>-1</sup> )<br>PCT: 0–10 ng mL <sup>-1</sup><br>(1 ng mL <sup>-1</sup> )                | 35   |
|             | cf DNA   | Epstein-Barr virus and bacteria           | Microneedle patch              | dCas9 and sgRNA  | Amperometric  | cfDNA: 30–30 000 fM (1.2 fM)  | 36   |
| Wound fluid | DNA/RNA  | <i>S. aureus</i> and <i>P. aeruginosa</i> | Microneedle patch              | NgAgo/gDNA   | Amperometric  | DNA/RNA: 0.3–300 fM (0.3 fM)  | 37   |
|             | DNA  | <i>S. aureus</i>                          | Hydrogel patch                 | Bacteria-responsive DNA hydrogel   | Capacitive  | <i>S. aureus</i> : 10 <sup>5</sup> –10 <sup>7</sup> CFU   | 62   |
|             | Inflammatory cytokines, bacterial load           | <i>S. aureus</i>                          | Bioanalytical dressing         | Aptamer  | EIS   | TNF-α: 0–2 ng mL <sup>-1</sup><br>IL-6: 0–30 ng mL <sup>-1</sup><br>IL-8: 0–30 ng mL <sup>-1</sup><br>TGF-β1: 0–150 pg mL <sup>-1</sup> | 63   |
|             | Glucose, lactate, uric acid, temperature, and pH | Infection                                 | Bioelectronic patch            | Glucose oxidase<br>Lactate oxidase<br>Uricase<br>Au microwire<br>pH<br>rGO/AuNPs | Amperometric<br>Amperometric<br>Amperometric<br>Resistance<br>Potentiometric<br>DPV | Glucose: 0–40 mM<br>Lactate: 0–4 mM<br>Uric acid: 0–150 µM<br>Temperature: 25–45 °C<br>pH: 4–8<br>Uric acid: 100–800 µM<br>(3.11 µM)    | 64   |
|             | Uric acid, temperature, pH                       | Infection                                 | Smart bandage                  | PANI<br>LMT70  | Potentiometric<br>Resistance  | pH: 3–9<br>Temperature: 25–45 °C  | 65   |
|             | Pyocyanin and pH                                 | <i>P. aeruginosa</i>                      | Bandage sensor array           | Porous CNT/graphene  | SWV   | Pyocyanin: 0.25–100 µM<br>(0.22 µM)   | 66   |
|             | DNA  | <i>S. aureus</i>                          | Paper-based wound dressing     | PANI/CNT<br>ZIF 67-C <sub>3</sub> N <sub>4</sub> nanocomposites and probe DNA    | Potentiometric<br>EIS   | pH: 6.0–10.0<br><i>S. aureus</i> target DNA: 1 fM–10 µM (0.46 fM)   | 67   |
|             | VOCs   | Infection                                 | Skin-interfaced chamber system | Commercial gas sensor (BME680, Bosch)  | Resistance  | fVOCs: 10 <sup>6</sup> –10 <sup>7</sup> mmol m <sup>-2</sup> h <sup>-1</sup>  | 68   |
|             | Bacteria burden                                  | <i>H. pylori</i>                          | Graphene nanosensor            | GBP-OHP  | Resistance  | <i>H. pylori</i> : 10 <sup>2</sup> –10 <sup>6</sup> cells (100 cells)   | 84   |
|             | Local salivary pH                                | Infection                                 | Dental patch                   | PANI   | Potentiometric  | pH: 3–8   | 85   |

Table 2 (continued)

| Biofluids | Biomarker                         | Microorganism                      | Platform          | Recognition element   | Mechanism                   | Linear range (LOD)  | Ref. |
|-----------|-----------------------------------|------------------------------------|-------------------|---|-----------------------------|---|------|
| Tears     | pH, glucose, protein, and nitrite | Infection                          | Contact lens      | pH-sensitive dyes<br>GOD/POD with TMB<br>3',3',5',5'-Tetrachlorophenol-3,4,5,6-tetrabromsulfophthalein<br>Azo dye | Colorimetric                | pH: 6.0–8.0 (pH: 0.25 pH units)<br>Glucose: 0–20 mmol L <sup>-1</sup> (1.84 mmol L <sup>-1</sup> )<br>Proteins: 0.5–5.0 g L <sup>-1</sup> (0.63 g L <sup>-1</sup> )<br>Nitrites: 10–200 μmol L <sup>-1</sup> (24.4 μmol L <sup>-1</sup> )<br>pH: 5.5–8.0<br>Protein: 0–10 g L <sup>-1</sup> | 91   |
|           | pH and total protein              | Corneal injury and dry-eye disease | Eye patch         | MR, BTB, PP, TBPP   | Colorimetric                |   | 11   |
|           | FQ                                | Infection                          | Eye patch         | Dual-emission fluorescent nanoprobes  | Fluorescence                | FQ antibiotics: 0–150 μM for each analyte (NOR, CIP, OFL, and LMF were 122, 164, 84, and 250 nM)<br>SARS-CoV-2: 500–100 000 copies, (500 copies)  | 92   |
| EBC       | Viral RNA                         | SARS-CoV-2, Ebola virus, and MRSA  | Face mask         | Toehold switches, aptamers, CRISPR-Cas12a complexes   | Colorimetric/fluorescence   |   | 95   |
|           | Viral spike protein               | SARS-CoV-2                         | Face mask         | Spike antibody  | Amperometric                | SARS-CoV-2 spike protein: 0.5 fg ml <sup>-1</sup> –1 pg ml <sup>-1</sup> (1 fg ml <sup>-1</sup> )   | 100  |
|           | VOCs                              | Coronavirus                        | Face mask         | Carbon nanoparticle electrode   | Amperometric/potentiometric | NO <sub>2</sub> : 0–2.5 μM, NH <sub>4</sub> <sup>+</sup> : 1–1000 μM  | 101  |
| Urine     | Nitrite                           | <i>E. coli</i>                     | Smart diaper      | Griess reagent  | Colorimetric                | Nitrite: 0–10 mg L <sup>-1</sup> (4 mg L <sup>-1</sup> )  | 111  |
|           | <i>E. coli</i> -specific enzyme   | <i>E. coli</i>                     | Urinary catheters | MUG and ONPG  | Fluorescence                | <i>E. coli</i> : 10 <sup>0</sup> –10 <sup>5</sup> CFU mL <sup>-1</sup> (1 CFU mL <sup>-1</sup> )  | 112  |

Abbreviations: rGO, reductive graphene oxide; AuNPs, gold nanoparticles; DPV, differential pulse voltammetry; PANI, polyaniline; LMT70, the temperature sensor chip; CNT, carbon nanotube; SWV, square wave voltammetry; EIS, electrochemical impedance spectroscopy; ZIF 67-C<sub>3</sub>N<sub>4</sub>, zeolitic imidazolate framework and carbon nitride; VOCs, volatile organic compounds; IP-10, interferon-inducible protein; TRAIL, tumor necrosis factor-related apoptosis-inducing ligand; CRP, C-reactive protein; cAbs, capture antibodies; dAb, detector antibody; GBP, graphene-binding peptide; OHP, odorrainin-HP; P/HRP2, *Plasmodium falciparum* histidine-rich protein 2; IgM/IgG, immunoglobulin M/immunoglobulin G; PCT, procalcitonin; LFA, lateral flow assay; cfdNA, cell-free DNA; dCas9, dead Cas9; sgrRNA, small guide RNA; CRISPR, clustered regularly interspaced short palindromic repeats; Cas9, CRISPR-associated protein 9; NgAgo, *Natronobacterium gregoryi* Argonaute; gDNA, genomic DNA; GOD-POD, glucose oxidase/peroxidase; TMB, tetramethylbenzidine; MR, methyl red; BTB, bromothymol blue; PP, phenolphthalein; TBPP, *tert*-butyl peroxybenzoate; FQ, fluoroquinolone; NOR, norfloxacin; CIP, ciprofloxacin; OFL, ofloxacin; LMF, lomefloxacin; MUG, methylumbelliferyl-β-D-glucuronide; ONPG, *ortho*-nitrophenyl-β-galactoside.



**Fig. 3** Wearable microfluidics for dermal fluid-based infection diagnosis. (a) SWEATSENSOR for electrochemical characterization of CRP and (b) the stable response of the SWEATSENSOR for IP-10 and TRAIL measurement.<sup>20</sup> (c) Sweat AWARE perspiration-based biosensing platform and (d) coefficient of determination ( $R^2$ ) of CRP.<sup>21</sup> (e) The mechanism of *in situ* microfluidic sweat CRP analysis and on-body multiplexed physicochemical analysis.<sup>22</sup> (f) Schematic of the CRISPR-Cas9 system and (g) the real-time *i-t* curve for detecting EBV cfDNA targets.<sup>36</sup> (h) Schematic of MN wearables on patients' epidermis for detection of cfDNA.<sup>37</sup> (i) Schematic of the wireless wound infection sensor WINDOW integrated with bioresponsive DNAgel and (j) *S. aureus* load at the wound site.<sup>62</sup> (k) Sensing mechanism of aptasensors for cytokines and bacteria and (l) the signal of *S. aureus* in serum.<sup>63</sup> (m) Schematic of a sensor array in iCares and (n) the multiplexed sensing responses upon adding target molecules.<sup>69</sup> Reproduced with permission from ref. 20 Copyright 2022, Wiley-VCH GmbH; ref. 21 Copyright 2024, Springer Nature; ref. 22 Copyright 2023, Springer Nature; ref. 36 Copyright 2022, Springer Nature; ref. 37 Copyright 2024, Springer Nature; ref. 62 Copyright 2021, American Association for the Advancement of Science; ref. 63 Copyright 2021, American Association for the Advancement of Science; ref. 69 Copyright 2025, American Association for the Advancement of Science.

bacterial sepsis *in vivo* for up to 10 days (Fig. 3f and g).<sup>36</sup> In a further refinement, a wireless patch incorporating prokaryotic Argonaute (NgAgo) tethered to DNA nanostructures enabled detection of DNA/RNA from *Staphylococcus aureus* and *Pseudomonas aeruginosa* (Fig. 3h).<sup>37</sup> Such advancements highlight the potential of microneedle systems for minimally invasive, continuous, and laboratory-free infection monitoring.

Wound exudate emerges as a critical biofluid for localized infection diagnostics, containing microbial DNA/RNA,<sup>38</sup> volatile organic compounds (VOCs),<sup>39–41</sup> microbial enzymes,<sup>42–46</sup> inflammatory cytokines,<sup>47–50</sup> acute-phase

proteins,<sup>51–53</sup> and metabolic markers.<sup>54–59</sup> Early identification of these biomarkers in wound fluid is crucial for timely intervention in infections and chronic wound management.<sup>60,61</sup> Devices such as the WINDOW sensor employ bioresponsive hydrogels to detect bacterial DNase activity, facilitating early-stage identification of wound infections (Fig. 3i and j).<sup>62</sup> Electrochemical smart dressings and battery-free smart bandages integrate multiplexed sensing of inflammatory cytokines (TNF- $\alpha$ , IL-6, IL-8, and TGF- $\beta$ 1), pH, temperature, and specific bacterial markers, allowing real-time diagnostics coupled with automated

therapeutic interventions (Fig. 3k and l).<sup>63–66</sup> A paper-based electrochemical dressing was used to detect *S. aureus* DNA in diabetic foot ulcers with high sensitivity and selectivity.<sup>67</sup> Non-contact wearable systems such as a sealed chamber further enhance wound diagnostics by analyzing VOCs and humidity with potential for wound monitoring.<sup>68</sup> Notably, a recent microfluidic smart bandage successfully collected wound exudate and performed *in situ* analysis of reactive species, and provided real-time biomarker monitoring and AI-assisted wound classification, demonstrating the translational promise of these approaches (Fig. 3m and n).<sup>69</sup>

## 2.2 Mucosal fluid-based infection diagnostics

Mucosal biofluids, particularly saliva and tears, offer easily accessible biomarkers for detecting oral, ocular, and systemic infections.<sup>70</sup> Saliva contains viral nucleic acids (RNA),<sup>71,72</sup> bacterial components,<sup>73,74</sup> inflammatory cytokines and chemokines,<sup>75–77</sup> immunoglobulins,<sup>78–80</sup> and metabolic biomarkers (Table 1).<sup>81–83</sup> Saliva-based sensors have been engineered for continuous monitoring of pathogens such as *Helicobacter pylori* using ultra-sensitive graphene nanosensors that detect the bacterial presence through conductivity changes (Fig. 4a and b).<sup>84</sup> Flexible dental patches provide real-time local pH measurements indicative of bacterial metabolic activity, enabling simultaneous monitoring and targeted therapeutic interventions (Fig. 4c and d).<sup>85</sup>

Tear fluid also contains pathogen-specific biomarkers, such as DNA/RNA, bacterial enzymes, microbial components,<sup>86,87</sup> immunoglobulins,<sup>88,89</sup> and proinflammatory cytokines during

ocular inflammation and systemic infections (Table 1).<sup>90</sup> These biomarkers have been utilized by wearable microfluidic contact lenses and epidermal patches. For example, a microfluidic contact lens enabled colorimetric sensing for pH, glucose, protein, and nitrite (Fig. 4e and f).<sup>91</sup> Similarly, an epidermal tear patch that detects vitamin C, calcium, pH, and total protein was developed.<sup>11</sup> Using colorimetric sensors and deep learning correction (CNN-GRU), the patch enabled accurate multi-analyte measurement from small tear volumes. While most tear-based wearables focus on host biomarkers, recent efforts have targeted therapeutic monitoring. Yin *et al.* developed a microfluidic eye patch integrating fluorescence sensors for detecting fluoroquinolone antibiotics in tears (Fig. 4g and h).<sup>92</sup> Tear-based sensing exemplifies the integration of minimally invasive sampling with advanced analytics to provide personalized and continuous healthcare insights.

## 2.3 Respiratory fluid-based diagnostics

Exhaled breath condensate (EBC) serves as a powerful noninvasive diagnostic medium that contains pathogen-specific VOCs,<sup>93,94</sup> nucleic acids,<sup>95,96</sup> and inflammatory markers relevant to respiratory infections and systemic diseases (Table 1). Systemic infections affect breath chemistry through elevated levels of PCT and CRP which are particularly relevant for sepsis and bacterial pneumonia.<sup>93,97,98</sup> Other VOCs, such as ketones, sulfur compounds, and alcohols, also shift during infection or gut dysbiosis, though further validation is needed.<sup>99</sup> Recent

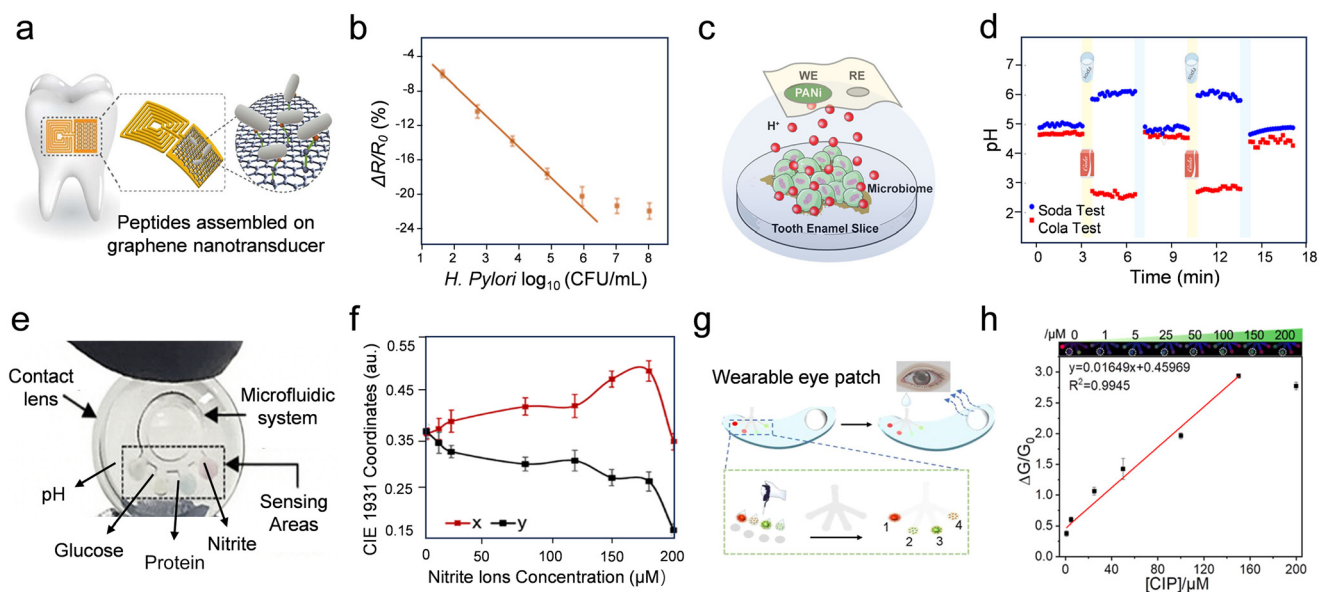


**Fig. 4** Wearable microfluidics for mucosal fluid-based infection diagnosis. (a) Schematic of a graphene wireless nanosensor on a tooth, and (b) the percentage of resistance change due to *H. pylori* cell recognition.<sup>84</sup> (c) pH monitoring of the *S. mutans* dental plaque formation process and (d) the pH test after drinking water, cola and soda.<sup>85</sup> (e) Schematic of a microfluidic contact lens and (f) the trend of the (x, y) coordinates at different nitrite levels.<sup>91</sup> (g) Schematic of the collection and detection of tears using an eye sensor patch and (h) the linearly fitted calibration curves of CIP.<sup>92</sup> Reproduced with permission from ref. 84 Copyright 2012, Springer Nature; ref. 85 Copyright 2022, Springer Nature; ref. 91 Copyright 2020, Elsevier B.V.; ref. 92 Copyright 2024, American Chemical Society.

developments, such as the CRISPR-based freeze-dried sensor embedded in wearable face masks, have enabled rapid detection of respiratory pathogens like SARS-CoV-2 directly from exhaled breath within minutes (Fig. 5a and b).<sup>95</sup> The system integrates a hydration reservoir,  $\mu$ PAD, and lateral flow strip for colorimetric readout and has been extended to detect Ebola and MRSA. Multifunctional bioelectronic masks, which combine aerosol immuno-capture, breath pattern analysis, and thermal monitoring, facilitate real-time diagnosis and severity assessment of SARS-CoV-2 respiratory diseases (Fig. 5c and d).<sup>100</sup> Integrated with machine learning, the system supports adaptation to formats like face masks, wristbands, and patches for continuous respiratory monitoring. Advances of a passive cooling system and a capillary-driven microfluidic network were developed to condense and analyze EBC. This system allows multi-analyte detection and analysis using the EBCare mask to track biomarkers, including ammonium, pH, and nitrite (Fig. 5e).<sup>101</sup> The system demonstrated robust performance in tracking the respiratory health status in conditions such as COPD, asthma, and post-COVID recovery.

## 2.4 Urine-based diagnostics

Urine, rich in biomarkers like nitrite, leukocyte esterase,<sup>102,103</sup> cytokines,<sup>104,105</sup> and microbial nucleic acids,<sup>106–108</sup> is essential for diagnosing urinary tract and systemic infections (Table 1).<sup>109,110</sup> Wearable urinary sensors, including smart diaper systems<sup>111</sup> and catheter-mounted biosensors,<sup>112</sup> enable automated and continuous detection of the bacterial presence. This self-powered

diaper system detected nitrite, outperforming standard dipstick tests, and is particularly suited for populations with limited communication, such as infants and elderly patients. The flexible catheter-mounted optical sensor mounted on a urine collection bag enabled real-time differentiation of pathogens like *Escherichia coli* from *Staphylococcus epidermidis* and *P. aeruginosa*, providing a continuous early-warning system for catheter-associated UTIs (Table 2). These wearable technologies provide early warnings for urinary tract infections, significantly improving patient outcomes, especially in vulnerable populations like infants and elderly individuals.

## 2.5 Challenges and future outlook

Despite advances in nanotechnology, intrinsic challenges remain for wearable sensing across different biofluids. For example, sweat analysis is still limited by the lack of knowledge regarding correlation with blood composition, low sample volume, and variable sweat secretion rates.<sup>113</sup> ISF monitoring faces issues with extraction efficiency, signal drift, and biological contamination at the MN interface. The long-term stability of ISF measurement requires overcoming the reliability issue and preventing irritation or infection.<sup>114</sup> Wound fluid is produced slowly and contains complex cellular, biofilm and enzymatic components which can clog microfluidic channels, hindering continuous infection monitoring. Saliva-based wearables also encounter limitations like irregular flow, complex composition, and biofouling from proteins and food debris.<sup>115</sup> Tears and breath condensate yield extremely low sample volumes and



**Fig. 5** Wearable microfluidics for respiratory fluid-based diagnosis. (a) Schematic of a wearable mask sensor integrated with a  $\mu$ PAD device, and (b) specificity study of the face-mask sensors.<sup>95</sup> (c) Structure, components, and multiple modules of PIDS for monitoring exhaled virus and (d) the statistical analysis of the current values obtained by a blow test and breath test of 42 volunteers.<sup>100</sup> (e) Schematic and sensing signals of the multiplexed wearable mask EBCare.<sup>101</sup> Reproduced with permission from ref. 95 Copyright 2021, Springer Nature; ref. 100 Copyright 2023, Springer Nature; ref. 101 Copyright 2024, American Association for the Advancement of Science.

analyte concentrations, making sensitivity and detection limits critical. Exhaled breath sensors must also resolve microbial volatiles from ambient background and humidity effectively. Each fluid thus requires specific engineering solutions for reliable microbial sensing.

Technological and analytical challenges include reliable fluid handling, long-term biocompatibility, and high analytical sensitivity. Advanced microfluidic designs and anti-fouling coatings are needed to achieve continuous, clog-free microfluidic flow, minimizing evaporation or contamination. Biocompatible, breathable materials are essential to avoid irritation over extended wear. To improve sensitivity and specificity of the sensing platform, integrated on-chip calibration and reference sensors are needed to help correct signal fluctuations. Multi-analyte sensing and cross-validation between biofluids are another strategy to confirm an infection signal. These approaches, together with more robust adhesives and miniaturized pumps, aim to produce wearable microfluidic systems that reliably monitor microbial biomarkers across diverse biofluids in real time.

### 3. Microorganisms as functional components in wearable microfluidic systems

Besides detecting microbial biomarkers, recent advances are now employing living microorganisms themselves as

functional components in wearable microfluidic platforms. These bio-integrated systems take advantage of the unique biological characteristics of engineered microorganisms, including their ability to sense environmental stimuli, generate biochemical outputs, and produce bioenergy. By combining synthetic biology and microfluidic technologies, microorganisms offer innovative solutions for environmental sensing, personalized diagnostics, and real-time health monitoring.

#### 3.1 Living biosensors for on-body sensing

Engineered microorganisms, including bacteria and yeast, have arisen as versatile biosensors due to their inherent sensitivity to biochemical signals and genetic programmability. For example, the development of a “living tattoo”, a wearable patch containing genetically engineered fluorescent *E. coli*, demonstrates the capacity for continuous biochemical monitoring directly on the skin (Fig. 6a).<sup>116</sup> Multiplexed detection of multiple analytes is supported by these bacterial biosensors, which respond dynamically to chemical stimuli. Similarly, *E. coli* encapsulated in protective hydrogels retained strong viability and sensing abilities for real-time identification of inflammation and microbial infections.<sup>117</sup> Because of their versatility for a range of sensing applications, yeast-based biosensors integrated into microfluidic chips have also demonstrated promise in environmental exposure monitoring, especially for the

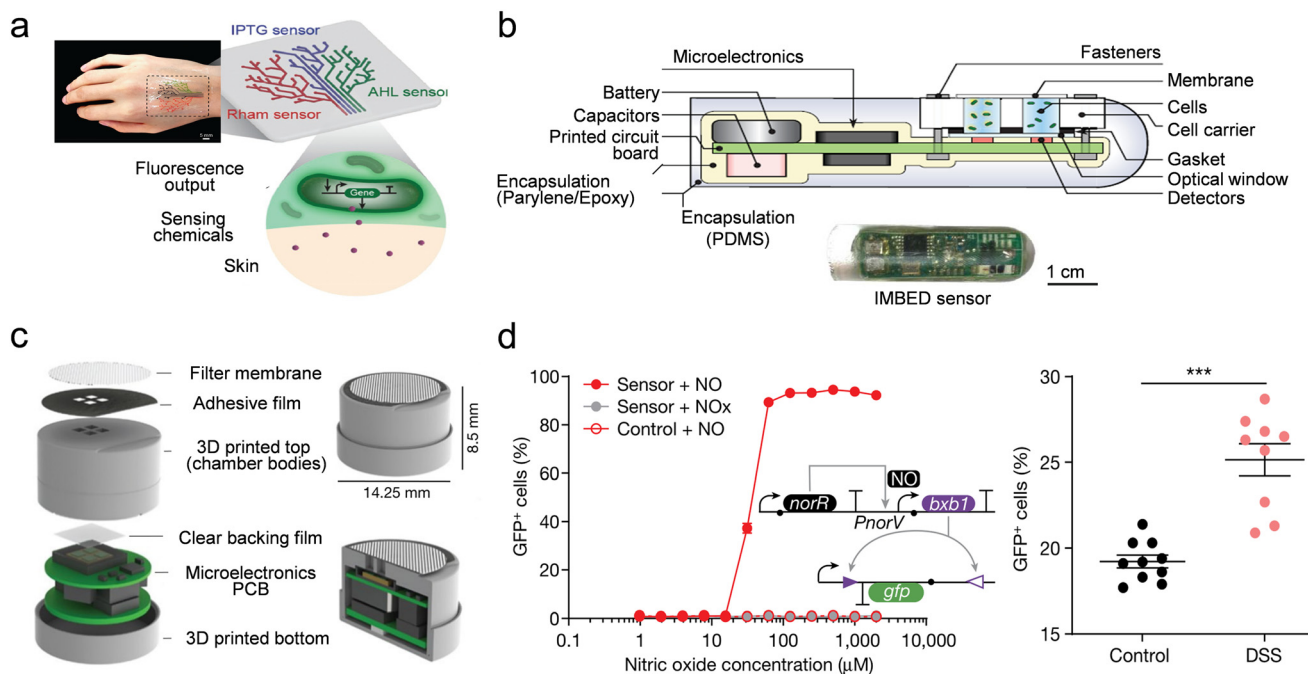


**Fig. 6** Microorganisms as functional components in wearable microfluidic systems. (a) The design of the living tattoo with different colors that respond to different chemicals by emitting fluorescence.<sup>116</sup> (b) Cross section and photo of the IMBED device.<sup>120</sup> (c) Design of a device for miniaturized wireless sensing with cell-based biosensors and (d) *in vitro* and *in vivo* validation of probiotic bacteria engineered to detect NO.<sup>121</sup> Reproduced with permission from ref. 116 Copyright 2018, Wiley-VCH GmbH; ref. 120 Copyright 2017, American Association for the Advancement of Science; ref. 121 Copyright 2023, Springer Nature.

detection of heavy metals.<sup>118,119</sup> However, there are still issues to be resolved, such as guaranteeing biosafety, preserving microbial viability in hostile environments, and resolving any potential regulatory hurdles related to genetically modified organisms.

### 3.2 Ingestible microbial diagnostic platforms

Integrating engineered microorganisms within ingestible devices represents a transformative approach to continuous gastrointestinal diagnostics. Microfluidic-electronic capsules containing engineered probiotic bacteria have been developed to detect gastrointestinal bleeding through heme sensing (Fig. 6b).<sup>120</sup> Upon biomarker detection, these microorganisms emit a detectable optical signal transmitted wirelessly to external monitoring devices. Another miniaturized device integrates genetically engineered probiotic biosensors with a custom photodetector and readout chip for real-time tracking of inflammation-associated signals in the gastrointestinal tract. The bacteria are genetically encoded to produce luminescence, enabling precise biological monitoring (Fig. 6c and d).<sup>121</sup> This method has major advantages over conventional diagnostic techniques and enables minimally invasive, real-time internal health monitoring. Further research has expanded this concept and demonstrated that microbial capsules can identify biomarkers of intestinal inflammation, leading to individualized internal diagnostics and the tracking of chronic gastrointestinal disorders.<sup>122</sup> Such systems highlight the potential for microorganisms as sensitive and selective internal biosensors within wearable and ingestible microfluidic platforms.

### 3.3 Challenges and future outlook

Utilizing living microorganisms in wearable biosensors introduces significant challenges related to stability, safety, and integration. Engineered microbial cells often lose function under variable wear conditions due to nutrient limitations, desiccation, or genetic drift. Without sufficient support, cell-based sensors may exhibit signal fluctuation or diminished sensitivity, reducing reproducibility.<sup>123</sup> Biosafety concerns include immune activation, horizontal gene transfer, and risks from accidental release. Integration into wearables also requires materials that preserve microbial viability while ensuring analyte diffusion and safe containment.<sup>124</sup> Response consistency is another issue, as biological sensors might have variable outputs between batches or individuals.

Future solutions include synthetic biology safeguards to enhance biocontainment and encapsulation in hydrogels or semipermeable membranes to stabilize microbes and prevent release. Cell-free systems, such as freeze-dried gene circuits, bypass viability constraints, stabilize responses and minimize noise while maintaining sensitive detection. In the future, one can envision mechanically and chemically tuned micro-bioreactors within wearables that preserve microbes under

optimal conditions, coupled with AI algorithms to interpret their signals. These approaches aim to deliver safe, robust, and reproducible microbial biosensors for continuous wear.

## 4. Microorganism-responsive therapeutics and smart treatment strategies

### 4.1 Microneedle systems for targeted delivery

Microneedle (MN) platforms provide real-time drug monitoring and targeted antimicrobial therapy in a minimally invasive manner. MNs enhance drug delivery to infected sites by rupturing biofilms and tissue barriers. For stimuli-responsive drug release, bacteria-triggered MNs only release drugs in the presence of infection. A lipase-responsive MN system uses microspheres to release antibiotics, such as doxycycline, upon sensing bacterial enzymes released from *S. aureus* or *P. aeruginosa*. Deferoxamine released from the hydrogel base promotes tissue regeneration, creating a dual-function therapeutic strategy (Fig. 7a and b).<sup>125</sup> Another approach incorporates magnetic nanoparticles into microneedles, generating localized hyperthermia to physically disrupt bacterial biofilms while releasing antioxidants to reduce inflammation and promote healing (Fig. 7c and d).<sup>126</sup>

Besides treating surface infections, advanced MN systems are being developed for immunomodulation in chronic diseases such as periodontal infections. MN patches sequentially release antibiotics and cytokines (IL-4, TGF- $\beta$ ) to eradicate bacterial pathogens and modulate immune responses for tissue repair (Fig. 7e and f).<sup>127</sup> For cutaneous leishmaniasis, MN-assisted skin pretreatment enhanced antifungal drug delivery.<sup>128</sup> Other targeted MN designs include ultrasound-responsive nanoparticle-loaded patches for treating *Propionibacterium acnes* infections, facilitating deep penetration and effective treatment of acne lesions.<sup>129</sup> Furthermore, electrochemical biosensors integrated into stainless-steel MNs provide continuous therapeutic monitoring of antibiotics, enabling real-time personalized dosing of antibiotics like vancomycin directly from interstitial fluid.<sup>130</sup> These examples illustrate the broad therapeutic versatility of MN systems in microbial disease management.

### 4.2 Intelligent bandages and advanced dressings

With the development of smart bandages and wound dressings, passive materials have been converted into multipurpose therapeutic systems that incorporate electronic actuation, biosensing, and responsive drug release. Smart bandages contain hydrogels that selectively react to infection-related *P. aeruginosa* lipases or *S. aureus*  $\alpha$ -hemolysin, while leaving commensal bacteria unaffected.<sup>131</sup> Other hydrogel systems respond to infection-related pH or enzyme cues to selectively activate antimicrobial delivery. Thermoresponsive hydrogels containing embedded microheaters offer wireless-controlled drug release when temperature elevations are related to infection.<sup>132</sup> Such systems combine sensor-driven



**Fig. 7** Wearable microfluidics for microorganism-responsive therapeutics. (a) The barrier destruction and wound healing mechanisms of Dox-DFO@MN Hy and (b) the bacterial response after releasing Dox.<sup>125</sup> (c) Schematic of the Fe-Se-HA MN based therapy for infected diabetic wounds and (d) the sterilization effect of MN patches.<sup>126</sup> (e) Antibacterial effect of MN patches and (f) the bacterial density after application of MNs.<sup>127</sup> (g) Illustration of cryoMNs for ocular delivery of predatory bacteria and (h) the time-dependent changes of *E. coli* concentrations after treatment.<sup>136</sup> Reproduced with permission from ref. 125 Copyright 2023, Wiley-VCH GmbH; ref. 126 Copyright 2023, Wiley-VCH GmbH; ref. 127 Copyright 2021, Elsevier B.V.; ref. 136 Copyright 2021, Wiley-VCH GmbH.

drug delivery with real-time physiological monitoring, exemplifying miniaturized closed-loop therapeutic strategies. Another wireless smart bandage with integrated sensors and stimulators could monitor temperature and impedance and deliver electrical stimulation.<sup>133</sup> Emerging wearable platforms, including microfluidic spinning fibers, flexible antibiotic pump patches, and drug-eluting contact lenses, further expand the toolkit for localized, responsive infection management.<sup>134,135</sup> These next-generation devices represent substantial progress toward wearable therapeutics that autonomously detect, respond, and adapt to clinical needs, and fully integrated on-body medical care.

#### 4.3 Bioengineered microbial and biologically-derived therapies

Biologically-derived therapies employ live microorganisms and bacteriophages to treat infections and prevent disease. One notable example is a cryomicroneedle patch that contains the predatory bacterium *Bdellovibrio bacteriovorus*, and is applied directly to infected ocular tissues. This method significantly reduces bacterial load through predation and achieves significant bacterial load reduction, highlighting the potential of 'living antibiotic' therapies that are highly specific and capable of self-amplification *via* direct delivery of live predatory bacteria (Fig. 7g and h).<sup>136</sup> Similarly, dressings loaded with bacteriophages show strong efficacy against pathogens resistant to antibiotics such as *Pseudomonas*, by efficiently breaking down biofilms and preserving localized antimicrobial activity.<sup>137</sup>

Dissolvable vaccine patches are another example of preventive applications. Patches delivering HPV and polio

vaccines have shown robust immune responses comparable to intramuscular injections, with advantages in stability and ease of administration for resource-limited settings.<sup>138,139</sup> Intramuscular injections are commonly associated with rapid systemic absorption and high peak concentration of a therapeutic agent. While this approach ensures nearly complete bioavailability and quick systemic exposure, it has drawbacks including injection site pain, infection risk, and less convenient repeat dosing. In contrast, transdermal drug delivery systems, such as skin patches, can provide a more sustained, controlled release of the therapeutic agent over time. Studies have shown that transdermal drug delivery can prolong the time to peak concentration and reduce concentration fluctuations compared to more immediate routes.<sup>140</sup>

#### 4.4 Challenges and future outlook

Microneedle-based wearables, smart dressings, and living microbial therapeutics face barriers to clinical translation. Device systems struggle with optimizing fluid sampling, sensor stability and biofouling, and integrating microfluidics with electronics and live components requires trade-offs in mechanical strength and biocompatibility. Manufacturing scale-up and regulatory classification are also uncertain hurdles. Living therapeutics pose unique safety concerns and off-target effects must be avoided. Notably, no engineered live biotherapeutic has yet earned regulatory approval, highlighting the difficulty of demonstrating consistent efficacy and safety in such emerging therapies.

Future directions focus on integrating advanced materials, synthetic biology, and AI to address these issues. Smart

delivery matrices like stimuli-responsive hydrogels are used to encapsulate therapeutic microbes for stability and on-demand release at infection sites.<sup>141</sup> Genetic safeguards are being designed to prevent uncontrolled microbe proliferation. Closed-loop microneedle patches and dressings with biosensors and machine learning can dynamically adjust phage or drug release based on real-time biomarker feedback. Researchers envision wearable platforms with interchangeable sensing and treatment units to tailor therapy to specific needs.

## 5. Integration of artificial intelligence in wearable microfluidic systems for microorganism detection and therapy

The increasing complexity of wearable biosensors generates extensive datasets, including continuous measurements from multiple biomarkers and physical parameters. AI such as machine learning (ML), deep learning (DL) and data fusion techniques is increasingly integrated into wearable and microfluidic systems and enables real-time signal interpretation, correction for physiological variability, and rapid classification of infection-related biomarkers.<sup>9</sup>

### 5.1 Machine learning for enhanced diagnostic precision

Machine learning offers powerful tools for identifying infection-related patterns in complex biological signals. For instance, wearable patches monitoring sweat cytokines (*e.g.*,

IP-10, TRAIL, and CRP) have employed cloud-based ML algorithms to distinguish bacterial *Mycoplasma pneumoniae* infections from viral infections such as COVID-19, delivering timely and accurate diagnostics.<sup>20</sup> A random forest model trained on key biomarkers like CRP, IL-6, and procalcitonin achieved high classification performance, demonstrating how algorithms can differentiate between types of bacterial and viral infections using biosensor data.<sup>142</sup> A skin-conformal microfluidic wound patch combined exudate analysis with ML-based pattern recognition to differentiate infection states in chronic wounds, supporting proactive treatment decisions.<sup>143</sup> Likewise, a 3D-printed epifluidic electronic skin integrated multimodal sensing and machine learning for continuous systemic health surveillance (Fig. 8a).<sup>144</sup> An all-flexible chronoepifluidic SERS patch applied autoencoder-driven quantification of sweat metabolites in real time (Fig. 8b).<sup>145</sup> In parallel, microneedle-microfluidic hybrids leverage hollow or porous microneedles for ISF sampling, where ML-guided spectral analysis enables accurate uric acid and glucose monitoring.<sup>146</sup> These advances demonstrate how wearable, microfluidic, and ML integration is moving diagnostics toward real-time, fluid-specific, and personalized infection monitoring. Importantly, such strategies can be extended to other fluids such as wound exudate, sweat, or saliva, supporting early detection and tailored interventions.

Predictive analytics through ML models, such as long short-term memory (LSTM) networks, have been effectively utilized for early-stage disease detection. For example, a hybrid CNN-LSTM model distinguished between different

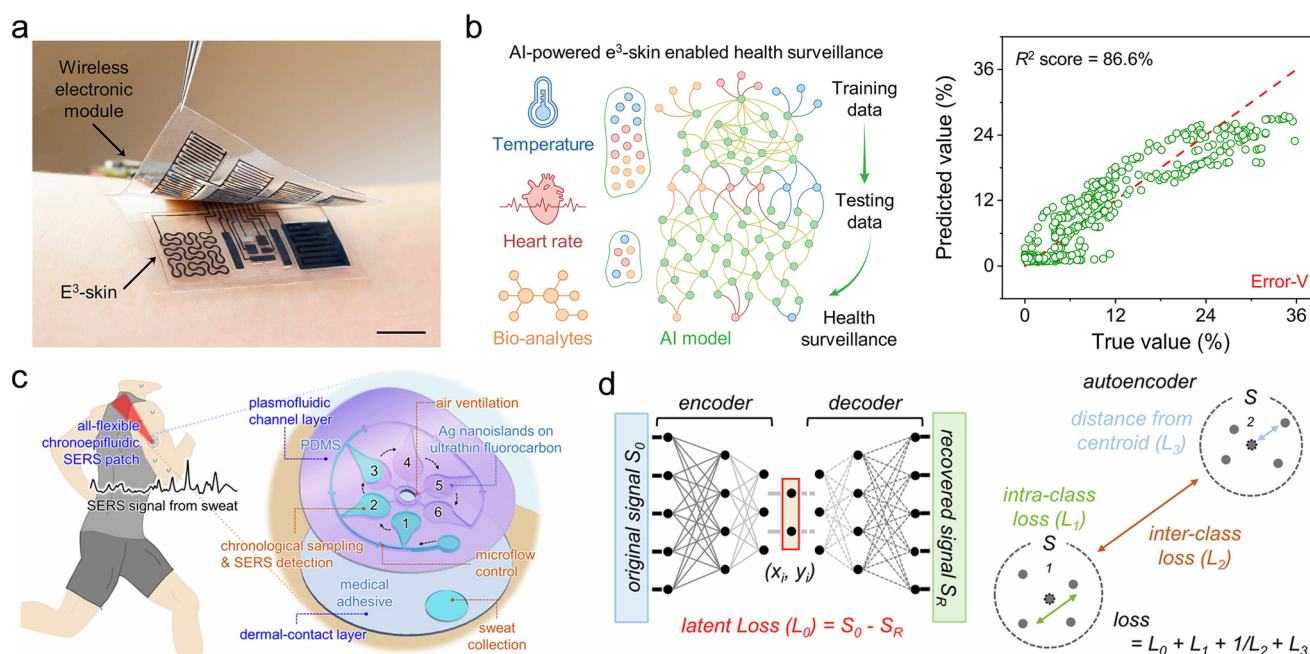


**Fig. 8** Integration of artificial intelligence in wearable microfluidic systems. (a) Optical images of an  $e^3$ -skin and a fully assembled wireless  $e^3$ -skin system and (b) the machine learning-powered multimodal  $e^3$ -skin for personalized health surveillance.<sup>144</sup> (c) Schematic illustration of an all-flexible chronoepifluidic SERS patch and (d) machine-learned metabolic quantification using an autoencoder combined with a logistic regression model.<sup>145</sup> Reproduced with permission from ref. 144 Copyright 2023, American Association for the Advancement of Science; ref. 145 Copyright 2025, Springer Nature.

types of lung diseases and predicted disease evolution.<sup>147</sup> Hybrid convolutional neural network–LSTM (CNN–LSTM) architectures can predict disease progression, offering significant clinical value by anticipating severe infection episodes before symptoms escalate.<sup>148,149</sup> Such predictive modeling can revolutionize personalized infection monitoring by identifying subtle yet critical physiological deviations unique to individual patients. Semi-supervised models have been used to identify deviations from individual baselines in the context of anomaly detection. Instead of depending on population-level thresholds, these methods allow for personalized monitoring.<sup>150</sup>

### 5.2 Multimodal data fusion and AI-optimized sensing

By combining chemical, physical, mechanical, and optical signals, wearable microfluidic devices naturally produce multimodal data streams. These various signals are combined by AI-driven multimodal data fusion to produce a thorough and precise diagnostic landscape.<sup>151</sup> Advanced dimensionality reduction techniques such as principal component analysis (PCA), t-distributed stochastic neighbor embedding (t-SNE), and autoencoder networks uncover intricate correlations among biomarkers and mechanical parameters, enhancing the interpretability of complex data.

Through the use of evolutionary algorithms and reinforcement learning, AI also optimizes sensor designs, examining a wide range of configurations to optimize robustness, performance, and sensitivity. Environmental variations, such as fluctuating sweat rates and temperature, can be enhanced by AI models to isolate clinically relevant microbial signals.<sup>152</sup> For example, autoencoder-based models, represented by architectures like AERed, significantly reduce computational load and energy consumption, enabling real-time data processing on resource-limited wearable platforms.<sup>153</sup> Recent work on stress-monitoring patches used a combination of sweat-rate sensing and machine learning to normalize biomarker levels for individual sweat rate differences, enabling more accurate assessments. Such multimodal fusion improves the accuracy and personalization of biosensing by compensating for physiological variability. Moreover, incorporating an AI-driven design framework has guided the development of optimization of the microchannel geometry to enable sensitive chemical detection and nanoparticle synthesis.<sup>154</sup> In such a way, AI could help design intricate channel networks that ensure consistent microorganism exposure to analytes and efficient sample transport.

### 5.3 AI-driven closed-loop therapeutic control

Integrating AI into wearable therapeutic systems enables intelligent, autonomous, and precise treatment delivery. When biosensors continuously detect infections or inflammation associated biomarkers, immediate therapeutic interventions are triggered such as localized antibiotic release or immunomodulatory drug delivery. AI algorithms

continuously monitor biomarker fluctuations and adapt therapeutic dosing and timing dynamically to achieve optimal outcomes. This concept of AI therapeutic control is already emerging. For example, prototypical closed-loop systems, such as glucose-responsive microneedle patches guided by AI, demonstrated successful autonomous glycemic regulation in diabetic models.<sup>155</sup> Applying this concept to infectious disease management could lead to intelligent wearable patches for early infection detection and treatment responses, such as antimicrobial delivery or biofilm disruption therapies.<sup>156</sup> This combination of real-time sensing, predictive analytics, and responsive therapeutics promises personalization and efficacy in infectious disease management.

### 5.4 Challenges and future outlook

Despite the promise of AI in enhancing wearable infection monitoring, technical and clinical barriers remain. Sensor heterogeneity, noise, and variability across users or devices complicate reliable data integration. Motion artifacts, missing values and environmental interference further degrade signal quality. Thus, AI models trained on limited datasets often fail to generalize across populations, leading to bias and performance loss.<sup>157</sup> Moreover, most algorithms function as “black boxes”, hindering clinician trust and raising concerns in high-risk infection monitoring. Privacy and security constraints also restrict centralized data sharing, limiting the diversity of training datasets and reducing robustness. These challenges highlight the need for rigorous model design, validation, and transparent outputs.

Future research should emphasize explainable AI to enhance transparency and clinician confidence, federated learning to preserve privacy while utilizing diverse datasets, and multimodal fusion architectures that integrate biochemical, physiological, and mechanical signals to improve predictive accuracy. Progress in data integration techniques enables the extraction of complementary features from multiple information streams, and validation is gradually moving toward prospective clinical trials and standardized benchmarks. These developments help to deliver AI-enabled wearables that are interpretable, privacy-preserving, and clinically validated, paving the way for integration into infection monitoring and personalized decision support.

## 6. Mechanomedicine in wearable microfluidic systems

Mechanomedicine explores how mechanical forces and the physical environment govern biological processes, recognizing that these cues influence biochemical signals in cell and microbial behaviors.<sup>158,159</sup> Recent advancements have recognized mechanomedicine as an innovative approach to wearable microfluidic systems, particularly in the area of infection diagnosis and therapeutic interventions,



**Fig. 9** AI-driven mechanodiagnosis, mechanobiology and mechanotherapies in wearable systems. In tissue-based mechanodiagnosis, AI algorithms can be used to capture biomechanical features for disease classification and prediction. Microfluidic platforms can simulate the physical microenvironment to study biofilm formation, antibiotic resistance, and cell and bacterial interaction. Mechanobiology-informed designs are used for effective infection detection and therapeutics. (a) Working principle of wound treatment by programmable and skin temperature-activated EMSDs.<sup>170</sup> (b) Overall schematics of hydrogel-enabled mechanically active healing of wounds.<sup>171</sup> Reproduced with permission from ref. 170 Copyright 2022, American Association for the Advancement of Science; ref. 171 Copyright 2023, Elsevier Ltd.

where tissues, fluids, and microbes all present measurable and actionable mechanics.

### 6.1 Diagnostic applications utilizing mechanical cues

In infectious diseases, pathogen activity and immune responses often alter tissue stiffness, edema pressure and biofluid rheology, such as increased tissue stiffness due to extracellular matrix remodeling or changes in fluid viscosity by inflammation response (Fig. 9).<sup>160</sup> These subtle changes could be detected by wearable microfluidic devices with integrated mechanical sensors to achieve timely and accurate infection diagnostics. For instance, wearable microfluidic bandages that track local pressure/stiffness can flag abscess formation or non-healing states. The microfluidic channels' hydrodynamics can sense biofluid viscosity changes where thickening of mucus may indicate respiratory infections for early alerts. Besides passive readouts, traction force signatures during epithelial closure are now mapped with traction microscopy.<sup>161</sup> Biochemical sensing in conjunction with mechanical diagnosis can boost diagnostic confidence and lower false positives.

### 6.2 Mechanobiology insights into host-microbe interactions

Pathogenic bacteria frequently form biofilms in tissue or on medical devices like catheters and implants under various mechanical conditions, such as fluid shear stress, compression, and extracellular matrix stiffness.<sup>162,163</sup> Microfluidic platforms, capable of simulating controlled shear environments, have significantly advanced the study of biofilm formation and antibiotic resistance (Fig. 9).<sup>164,165</sup> For instance, bacteria such as *S. aureus* and *P. aeruginosa* exhibit increased adherence and biofilm robustness under higher shear conditions.<sup>160,166</sup> Wearable microfluidic devices designed with periodic mechanical stimuli, such as microfluidic pulses or acoustic vibrations, can exploit these insights to disrupt microbial early attachment and reduce infection risk.<sup>167,168</sup>

Moreover, mechanical stimuli also profoundly influence immune cell function and microbial virulence gene expression. Lung pathogens, for instance, respond to mechanical cues such as cyclic stretch from breathing, modulating their virulence pathways.<sup>169</sup> The human gut experiences rhythmic contractions and fluid shear from flow

of contents.<sup>164</sup> Microfluidic organ-on-chip models that replicate these physiological mechanical dynamics have demonstrated their value in capturing realistic host–microbe interactions, indicating the importance of mechanobiology-informed designs for effective infection detection and therapeutic strategies.

### 6.3 Emerging mechanotherapies in wearable systems

Wearable microfluidic platforms integrated with mechanotherapy offer new therapeutic opportunities that complement traditional chemical treatments. Wearable microfluidics are increasingly active rather than passive. A skin temperature activated device could improve the closure rates and promote reepithelialization by upregulating EGF, VEGF, and TGF- $\beta$  expression, demonstrating synergistic mechanotherapy and electrotherapy for wound healing (Fig. 9a).<sup>170</sup> Hydrogel-based mechanically active dressings apply inward contractile forces to wound edges, improving closure compared to passive coverings (Fig. 9b).<sup>171</sup> Mechanically gated microfluidics also enable sampling that is useful for point-of-care diagnostics. For example, a pressure-triggered microfluidic contact lens uses blink-generated forces to open a check valve for controllable release of antibiotics in tears without electronics.<sup>172</sup> Together with concepts like vibration or ultrasound micro-actuation to disrupt biofilms using wearable smart wound patches and deformation-responsive hydrogels that release drugs upon stretch, these systems indicate opportunities of combining mechanical and biochemical interventions within wearable systems to provide an overall approach to infection treatment.<sup>173</sup>

### 6.4 Challenges and future outlook

The incorporation of mechanobiology into wearable microfluidic systems is still emerging, and several challenges remain. The first is to understand and measure mechanical cues *in vivo*, such as how force shifts affect microbes and host tissues, but current wearables rarely capture such mechanical cues. Another challenge is the knowledge gap in understanding the response of microbial communities to mechanical cues. Methods are still lacking to systematically study how varied mechanical cues affect virulence, growth, and biofilm integrity of different pathogens. Other challenges include safe integration of mechanical actuators into wearables, and the complexation of coupling between mechanical and biochemical signals.

Future directions include bioinspired soft actuators that deliver safe, controlled forces, and microfluidic mechanoscreening platforms that probe microbial and host responses under varied mechanical conditions. Engineering mechanosensitive microbial reporters may provide real-time readouts of local forces, while closed-loop systems could combine vibration or ultrasound with antibiotic release to synergistically disrupt biofilms. Integrating mechanosensing, mechano-actuation, and biochemical analytics within

wearable platforms could create multimodal systems that detect infection-related biomechanical signatures and deliver targeted mechanotherapeutic interventions, which help advance infection management beyond conventional biochemical sensing.

## 7. Conclusions and future perspectives

The rapid advancements in wearable microfluidic systems have opened new frontiers in personalized healthcare for infectious diseases by enabling continuous, minimally invasive monitoring and responsive therapeutic interventions. Current wearable technologies effectively make use of diverse human biofluids, including sweat, saliva, interstitial fluid, tears, breath, urine, and wound exudate, for real-time detection of microbial and host-derived biomarkers. Future innovations will focus on integrating multi-fluid and multimodal sensing platforms, allowing comprehensive and cross-validated infection monitoring, significantly reducing diagnostic uncertainty.

The integration of AI with wearable microfluidics holds great promise to greatly improve infection diagnostics and therapy. AI-driven analytics enable wearable devices to accurately interpret complex physiological and biochemical signals, adjusting dynamically to individual patient baselines and environmental variations. Nonetheless, such microorganism-integrated wearable platforms still face critical system-level gaps. Robust machine-learning models will require extensive training on diverse patient data to ensure accuracy and generalizability, and careful attention must be paid to data security and patient privacy in handling the biosensor data. Advances in flexible electronics, bioresorbable materials, and stable microfluidic architectures will be important in translating these devices from laboratory prototypes into broadly accessible clinical tools. Regulatory strategies for AI-driven diagnostic devices are still emerging, and transparent algorithms and thorough validation will be needed to gain clinical approval.

Mechanomedicine insights into how mechanical cues influence microbe–sensor interactions remain underexplored, limiting incorporation of biomechanical and mechanobiological information for diagnostic and therapeutic applications. Scalable and sustainable manufacturing methods, and biocompatible and mechanically robust materials are needed. Future wearable devices will likely combine biochemical and mechanical sensing, bringing insights from tissue stiffness, biofluid viscosity, and dynamic microbial environments to enhance diagnostic precision. Integration of mechanomedicine principles into wearable microfluidics will also facilitate innovative therapeutic modalities, such as mechanically responsive hydrogels or actuators that disrupt pathogenic biofilms or modulate local tissue responses.

In conclusion, AI-driven wearable microfluidic systems integrating microorganisms and mechanomedicine



**Fig. 10** Toward intelligent wearables integrating mechanomedicine for infection management. This conceptual diagram illustrates the integration of micro-mechanical insights, multi-fluid sensing, and AI analytics in next-generation wearable devices. In diverse infection contexts, the physical microenvironment influences both microbial behavior and host responses, leading to unique mechano-biomarkers alongside biochemical markers. Wearable microfluidic platforms interface with the body at these sites to continuously sample biofluids and monitor signals of infection. The data streams from these devices are fed into an AI-driven analysis that performs real-time noise filtering, pattern recognition, and even predictive analytics. Through cloud connectivity, these wearables enable telemedicine and global health surveillance.

principles offer transformative potential for infection diagnosis, therapy, and health management (Fig. 10). Interdisciplinary collaboration among engineers, microbiologists, clinicians, data scientists, and regulatory experts will be required to realize these next-generation wearable devices. With sustained effort, wearable technologies can fundamentally shift infectious disease management toward prevention, early intervention, and personalized care, significantly improving global health outcomes.

## Author contributions

F. Xu and K. Qu conceived the idea and outlined the project. Y. Zhou and X. Y. Zhu conducted the original literature study and wrote the manuscript draft. All authors contributed to the writing of the manuscript and approved the manuscript.

## Conflicts of interest

The authors declare no conflicts of interest.

## Data availability

No primary research results, software, or code have been included and no new data were generated or analyzed as part of this review.

## Acknowledgements

We gratefully acknowledge the financial support from the National Natural Science Foundation of China (12432015), the Key Research and Development Projects of Shaanxi Province of China (2023GXLH-033), the Shaanxi Fundamental Science Research Project for Chemistry & Biology (22JHQ060), and the Natural Science Basic Research Program of Shaanxi Province of China (2024JC-YBQN-0122). The figures in this article were created using BioRender.

## References

- 1 D. Prakashan, R. P. R. and S. Gandhi, *Diagnostics*, 2023, **13**, 916.
- 2 G. Chen, S. Shen, T. Tat, X. Zhao, Y. Zhou, Y. Fang and J. Chen, *View*, 2022, **3**, 20220024.
- 3 J. Kim, A. S. Campbell and J. Wang, *Talanta*, 2018, **177**, 163–170.
- 4 X. Wang, X. Z. Hong, Y. W. Li, Y. Li, J. Wang, P. Chen and B. F. Liu, *Mil. Med. Res.*, 2022, **9**, 11.
- 5 T. Lehnert and M. A. M. Gijs, *Lab Chip*, 2024, **24**, 1441–1493.
- 6 Y. Fang, X. Zhao, T. Tat, X. Xiao, G. Chen, J. Xu and J. Chen, *Matter*, 2021, **4**, 1102–1105.
- 7 X. Zhang, Y. Wang, J. Chi and Y. Zhao, *Research*, 2020, **2020**, 7462915.

- 8 Y. Li, C. Xu, Y. Liao, X. Chen, J. Chen, F. Yang and M. Gao, *Biomicrofluidics*, 2024, **18**, 061303.
- 9 A. M. Zeid, I. M. Mostafa, B. Lou and G. Xu, *Lab Chip*, 2023, **23**, 4160–4172.
- 10 S. Shajari, K. Kuruvinishetti, A. Komeili and U. Sundararaj, *Sensors*, 2023, **23**, 9498.
- 11 Z. Wang, Y. Dong, X. Sui, X. Shao, K. Li, H. Zhang, Z. Xu and D. Zhang, *npj Flexible Electron.*, 2024, **8**, 35.
- 12 R. Oria, K. Jain and V. M. Weaver, *npj Biol. Phys. Mech.*, 2025, **2**, 9.
- 13 J. P. H. Wong, M. Fischer-Stettler, S. C. Zeeman, T. J. Battin and A. Persat, *Proc. Natl. Acad. Sci. U. S. A.*, 2023, **120**, e2217577120.
- 14 A. Parihar, S. Yadav, M. A. Sadique, P. Ranjan, N. Kumar, A. Singhal, V. Khare, R. Khan, S. Natarajan and A. K. Srivastava, *Bioeng. Transl. Med.*, 2023, **8**, e10481.
- 15 B. Jagannath, K. C. Lin, M. Pali, D. Sankhala, S. Muthukumar and S. Prasad, *Bioeng. Transl. Med.*, 2021, **6**, e10220.
- 16 K. Song, Y. Chen, R. Göke, A. Wilmen, C. Seidel, A. Göke, B. Hilliard and Y. Chen, *J. Exp. Med.*, 2000, **191**, 1095–1104.
- 17 O. Schildgen, K. Oved, A. Cohen, O. Boico, R. Navon, T. Friedman, L. Etshtein, O. Kriger, E. Bamberger, Y. Fonar, R. Yacovov, R. Wolchinsky, G. Denkberg, Y. Dotan, A. Hochberg, Y. Reiter, M. Grupper, I. Srugo, P. Feigin, M. Gorfine, I. Chistyakov, R. Dagan, A. Klein, I. Potasman and E. Eden, *PLoS One*, 2015, **10**, e0120012.
- 18 R. W. Johnstone, A. J. Frew and M. J. Smyth, *Nat. Rev. Cancer*, 2008, **8**, 782–798.
- 19 B. Jagannath, K. C. Lin, M. Pali, D. Sankhala, S. Muthukumar and S. Prasad, *Inflammatory Bowel Dis.*, 2020, **26**, 1533–1542.
- 20 B. Jagannath, M. Pali, K. C. Lin, D. Sankhala, P. Naraghi, S. Muthukumar and S. Prasad, *Adv. Mater. Technol.*, 2022, **7**, 2101356.
- 21 B. C. Davis, K. C. Lin, S. Shahub, A. Ramasubramanya, A. Fagan, S. Muthukumar, S. Prasad and J. S. Bajaj, *NPJ Digit. Med.*, 2024, **7**, 382.
- 22 J. Tu, J. Min, Y. Song, C. Xu, J. Li, J. Moore, J. Hanson, E. Hu, T. Parimon, T. Y. Wang, E. Davoodi, T. F. Chou, P. Chen, J. J. Hsu, H. B. Rossiter and W. Gao, *Nat. Biomed. Eng.*, 2023, **7**, 1293–1306.
- 23 S. Ma, J. Li, L. Pei, N. Feng and Y. Zhang, *J. Pharm. Anal.*, 2023, **13**, 111–126.
- 24 X. Zhang, W. Zhang, W. Wu and J. Chen, *Microchem. J.*, 2023, **195**, 109477.
- 25 Y. Hu, Y. Zhao, Y. Zhang, W. Chen, H. Zhang and X. Jin, *Trends Microbiol.*, 2025, **33**, 421–433.
- 26 X. Wang, M. R. Lennartz, D. J. Loegering and J. A. Stenzen, *Cytokine*, 2008, **43**, 15–19.
- 27 P. R. Miller, R. M. Taylor, B. Q. Tran, G. Boyd, T. Glaros, V. H. Chavez, R. Krishnakumar, A. Sinha, K. Poorey, K. P. Williams, S. S. Branda, J. T. Baca and R. Polsky, *Commun. Biol.*, 2018, **1**, 173.
- 28 J. J. García-Guzmán, C. Pérez-Ráfols, M. Cuartero and G. A. Crespo, *ACS Sens.*, 2021, **6**, 1129–1137.
- 29 T. Siegmund, L. Heinemann, R. Kolassa and A. Thomas, *J. Diabetes Sci. Technol.*, 2017, **11**, 766–772.
- 30 R. Mei, Y. Wang, S. Shi, X. Zhao, Z. Zhang, X. Wang, D. Shen, Q. Kang and L. Chen, *Anal. Chem.*, 2022, **94**, 16069–16078.
- 31 K. E. Poti, D. J. Sullivan, A. M. Dondorp and C. J. Woodrow, *Trends Parasitol.*, 2020, **36**, 112–126.
- 32 E. C. Wilkerson, D. Li and P. B. Lillehoj, *ACS Sens.*, 2024, **9**, 5792–5801.
- 33 F. Ribet, A. Bendes, C. Fredolini, M. Dobielewski, M. Böttcher, O. Beck, J. M. Schwenk, G. Stemme and N. Roxhed, *Adv. Healthcare Mater.*, 2023, **12**, 2202564.
- 34 X. Jiang and P. B. Lillehoj, *Microsyst. Nanoeng.*, 2020, **6**, 96.
- 35 J. G. Turner, E. Lay, U. Jungwirth, V. Varenko, H. S. Gill, P. Estrela and H. S. Leese, *Adv. Mater. Technol.*, 2023, **8**, 2300259.
- 36 B. Yang, J. Kong and X. Fang, *Nat. Commun.*, 2022, **13**, 3999.
- 37 B. Yang, H. Wang, J. Kong and X. Fang, *Nat. Commun.*, 2024, **15**, 1936.
- 38 S. B. Mudaliar and A. S. Bharath Prasad, *World J. Microbiol. Biotechnol.*, 2024, **40**, 90.
- 39 M. Azimzadeh, P. Khashayar, M. Mousazadeh, M. Daneshpour, M. Rostami, D. R. Goodlett, K. Manji, S. Fardindoost, M. Akbari and M. Hoorfar, *Talanta*, 2025, **292**, 127991.
- 40 C. E. Chitnis, L. D. J. Bos, P. J. Sterk and M. J. Schultz, *PLoS Pathog.*, 2013, **9**, e1003311.
- 41 A. N. Thomas, S. Riazanskaia, W. Cheung, Y. Xu, R. Goodacre, C. L. P. Thomas, M. S. Baguneid and A. Bayat, *Wound Repair Regen.*, 2010, **18**, 391–400.
- 42 L. Lauková, B. Konečná, E. Janovičová, B. Vlková and P. Celec, *Biomolecules*, 2020, **10**, 1036.
- 43 P. Chandra, Enespa, R. Singh and P. K. Arora, *Microb. Cell Fact.*, 2020, **19**, 169.
- 44 T. Fu, P. Stupnitskaia and S. Matoori, *ACS Meas. Sci. Au*, 2022, **2**, 377–384.
- 45 V. Thammavongsa, D. M. Missiakas and O. Schneewind, *Science*, 2013, **342**, 863–866.
- 46 J. Garcia Gonzalez and F. J. Hernandez, *Expert Rev. Mol. Diagn.*, 2022, **22**, 265–294.
- 47 S. Liarte, Á. Bernabé-García and F. J. Nicolás, *Cell*, 2020, **9**, 306.
- 48 G. S. Ashcroft, M. J. Jeong, J. J. Ashworth, M. Hardman, W. Jin, N. Moutsopoulos, T. Wild, N. McCartney-Francis, D. Sim, G. McGrady, X. y. Song and S. M. Wahl, *Wound Repair Regen.*, 2011, **20**, 38–49.
- 49 Y. Wu, M. Wang, Y. Zhu and S. Lin, *Medicine*, 2016, **95**, e5127.
- 50 F. Mannello, D. Ligi, M. Canale and J. D. Raffetto, *Expert Rev. Mol. Diagn.*, 2014, **14**, 737–762.
- 51 T. W. Du Clos, *Ann. Med.*, 2009, **32**, 274–278.
- 52 Y.-y. Luan, C.-h. Yin and Y.-m. Yao, *Front. Immunol.*, 2021, **12**, 720363.
- 53 G. Shabestani Monfared, P. Ertl and M. Rothbauer, *Pharmaceutics*, 2021, **13**, 793.
- 54 M. Galliani, C. Diacci, M. Berto, M. Sensi, V. Beni, M. Berggren, M. Borsari, D. T. Simon, F. Biscarini and C. A. Bortolotti, *Adv. Mater. Interfaces*, 2020, **7**, 2001218.

- 55 Y. Wang, Y. Liu, G. Xiang, Y. Jian, Z. Yang, T. Chen, X. Ma, N. Zhao, Y. Dai, Y. Lv, H. Wang, L. He, B. Shi, Q. Liu, Y. Liu, M. Otto and M. Li, *Nat. Commun.*, 2024, **15**, 9835.
- 56 D. G. Metcalf, M. Haalboom, P. G. Bowler, C. Gamerith, E. Sigl, A. Heinzle and M. W. M. Burnet, *Wound Medicine*, 2019, **26**, 100166.
- 57 Q. Pang, D. Lou, S. Li, G. Wang, B. Qiao, S. Dong, L. Ma, C. Gao and Z. Wu, *Adv. Sci.*, 2020, **7**, 1902673.
- 58 M. Dong, X. Sun, L. Li, K. He, J. Wang, H. Zhang and L. Wang, *J. Colloid Interface Sci.*, 2022, **610**, 913–922.
- 59 J. V. Boykin, *J. Wound Ostomy Cont. Nurs.*, 2010, **37**, 25–32.
- 60 A. Uberoi, A. McCready-Vangi and E. A. Grice, *Nat. Rev. Microbiol.*, 2024, **22**, 507–521.
- 61 A. Laliwala, A. Pant, D. Svehkarev, M. R. Sadykov and A. M. Mohs, *NPJ Biosens.*, 2024, **1**, 17.
- 62 Z. Xiong, S. Achavananthadith, S. Lian, L. E. Madden, Z. X. Ong, W. Chua, V. Kalidasan, Z. Li, Z. Liu, P. Singh, H. Yang, S. P. Heussler, S. M. P. Kalaiselvi, M. B. H. Breese, H. Yao, Y. Gao, K. Sanmugam, B. C. K. Tee, P. Y. Chen, W. Loke, C. T. Lim, G. S. H. Chiang, B. Y. Tan, H. Li, D. L. Becker and J. S. Ho, *Sci. Adv.*, 2021, **7**, eabj1617.
- 63 Y. Gao, D. T. Nguyen, T. Yeo, S. B. Lim, W. X. Tan, L. E. Madden, L. Jin, J. Y. K. Long, F. A. B. Aloweni, Y. J. A. Liew, M. L. L. Tan, S. Y. Ang, S. D. Maniya, I. Abdelwahab, K. P. Loh, C. H. Chen, D. L. Becker, D. Leavesley, J. S. Ho and C. T. Lim, *Sci. Adv.*, 2021, **7**, eabg9614.
- 64 E. Shirzaei Sani, C. Xu, C. Wang, Y. Song, J. Min, J. Tu, S. A. Solomon, J. Li, J. L. Banks, D. G. Armstrong and W. Gao, *Sci. Adv.*, 2023, **9**, eadf7388.
- 65 G. Xu, Y. Lu, C. Cheng, X. Li, J. Xu, Z. Liu, J. Liu, G. Liu, Z. Shi, Z. Chen, F. Zhang, Y. Jia, D. Xu, W. Yuan, Z. Cui, S. S. Low and Q. Liu, *Adv. Funct. Mater.*, 2021, **31**, 2100852.
- 66 K. Kaewpradub, K. Veenuttranon, H. Jantapaso, P. Mittraparp-Arthorn and I. Jeerapan, *Nano-Micro Lett.*, 2024, **17**, 71.
- 67 S. Roy, K. Bisaria, S. Nagabooshanam, A. Selvam, S. Chakrabarti, S. Wadhwa, R. Singh, A. Mathur and J. Davis, *IEEE Sens. J.*, 2021, **21**, 1215–1221.
- 68 J. Shin, J. W. Song, M. T. Flavin, S. Cho, S. Li, A. Tan, K. R. Pyun, A. G. Huang, H. Wang, S. Jeong, K. E. Madsen, J. Trueb, M. Kim, K. Nguyen, A. Yang, Y. Hsu, W. Sung, J. Lee, S. Phyo, J. H. Kim, A. Banks, J. K. Chang, A. S. Paller, Y. Huang, G. A. Ameer and J. A. Rogers, *Nature*, 2025, **640**, 375–383.
- 69 C. Wang, K. Fan, E. Shirzaei Sani, J. A. Lasalde-Ramírez, W. Heng, J. Min, S. A. Solomon, M. Wang, J. Li, H. Han, G. Kim, S. Shin, A. Seder, C.-D. Shih, D. G. Armstrong and W. Gao, *Sci. Transl. Med.*, 2025, **17**, eadt0882.
- 70 L. C. P. M. Schenkels, E. C. I. Veerman and A. V. N. Amerongen, *Crit. Rev. Oral Biol. Med.*, 1995, **6**, 161–175.
- 71 S. S. Chandrasekaran, S. Agrawal, A. Fanton, A. R. Jangid, B. Charrez, A. M. Escajeda, S. Son, R. McIntosh, H. Tran, A. Bhuiya, M. D. de León Derby, N. A. Switz, M. Armstrong, A. R. Harris, N. Prywes, M. Lukarska, S. B. Biering, D. C. J. Smock, A. Mok, G. J. Knott, Q. Dang, E. Van Dis, E. Dugan, S. Kim, T. Y. Liu, J. R. Hamilton, E. Lin-Shiao, E. C. Stahl, C. A. Tsuchida, P. Giannikopoulos, M. McElroy, S. McDevitt, A. Zur, I. Sylvain, A. Ciling, M. Zhu, C. Williams, A. Baldwin, E. A. Moehle, K. Kogut, B. Eskenazi, E. Harris, S. A. Stanley, L. F. Lareau, M. X. Tan, D. A. Fletcher, J. A. Doudna, D. F. Savage, P. D. Hsu and I. G. I. T. Consortium, *Nat. Biomed. Eng.*, 2022, **6**, 944–956.
- 72 A. Sueki, K. Matsuda, A. Yamaguchi, M. Uehara, M. Sugano, T. Uehara and T. Honda, *Clin. Chim. Acta*, 2016, **453**, 71–74.
- 73 D.-H. Baek and S.-H. Lee, *J. Microbiol. Biotechnol.*, 2023, **33**, 998–1005.
- 74 C. Liu, N. Yazdani, C. S. Moran, C. Salomon, C. J. Seneviratne, S. Ivanovski and P. Han, *Acta Biomater.*, 2024, **180**, 18–45.
- 75 H. E. Davis, L. McCorkell, J. M. Vogel and E. J. Topol, *Nat. Rev. Microbiol.*, 2023, **21**, 133–146.
- 76 H. A. Alwafi, S. S. Ali, S. B. Kotha, L. W. Abuljadayel, M. Ibrahim, I. R. N. Elahi, H. A. Alwafi, M. S. Almuhayawi, M. D. Finkelman and N. A. El-Shitany, *Can. J. Infect. Dis. Med. Microbiol.*, 2022, **2022**, 1543918.
- 77 D. Belstrøm, C. Damgaard, E. Könönen, M. Gürsoy, P. Holmstrup and U. K. Gürsoy, *J. Oral Microbiol.*, 2017, **9**, 1364101.
- 78 A. Mousavizadeh, B. Afroozi, F. Hadinia, M. Azarshab and A. Hadinia, *Clin. Lab.*, 2021, **67**, DOI: [10.7754/Clin.Lab.2020.201209](https://doi.org/10.7754/Clin.Lab.2020.201209).
- 79 A. Niedźwiedź, E. Pius-Sadowska, M. Kawa, A. Kuligowska, M. Parczewski, K. Safranow, K. Kozłowski, B. Machaliński and A. Machalińska, *Pathogens*, 2022, **11**, 1098.
- 80 E. Ito, K. Tsukinoki, T. Yamamoto, K. Handa, M. Iwamiya, J. Saruta, S. Ino and T. Sakurai, *PLoS One*, 2021, **16**, e0249979.
- 81 T. Kadota, M. Hamada, R. Nomura, Y. Ogaya, R. Okawa, N. Uzawa and K. Nakano, *Biomedicines*, 2020, **8**, 161.
- 82 D. Kim, J. P. Barraza, R. A. Arthur, A. Hara, K. Lewis, Y. Liu, E. L. Scisci, E. Hajishengallis, M. Whiteley and H. Koo, *Proc. Natl. Acad. Sci. U. S. A.*, 2020, **117**, 12375–12386.
- 83 K. V. S. H. Kumar, M. Saini, U. Kapoor and P. Banga, *Indian J. Endocrinol. Metab.*, 2012, **16**, 664–665.
- 84 M. S. Mannoor, H. Tao, J. D. Clayton, A. Sengupta, D. L. Kaplan, R. R. Naik, N. Verma, F. G. Omenetto and M. C. McAlpine, *Nat. Commun.*, 2012, **3**, 763.
- 85 Z. Shi, Y. Lu, S. Shen, Y. Xu, C. Shu, Y. Wu, J. Lv, X. Li, Z. Yan, Z. An, C. Dai, L. Su, F. Zhang and Q. Liu, *npj Flexible Electron.*, 2022, **6**, 49.
- 86 Y. T. Wu, C. Tam, L. S. Zhu, D. J. Evans and S. M. J. Fleiszig, *Ocul. Surf.*, 2017, **15**, 88–96.
- 87 D. R. Blais, S. G. Vascotto, M. Griffith and I. Altosaar, *Invest. Ophthalmol. Visual Sci.*, 2005, **46**, 4235–4244.
- 88 A. M. McDermott, *Exp. Eye Res.*, 2013, **117**, 53–61.
- 89 Y. X. Chao, O. Röttschke and E.-K. Tan, *Brain, Behav., Immun.*, 2020, **87**, 182–183.
- 90 T. Yamaguchi, B. M. Calvacanti, A. Cruzat, Y. Qazi, S. Ishikawa, A. Osuka, J. Lederer and P. Hamrah, *Invest. Ophthalmol. Visual Sci.*, 2014, **55**, 7457–7466.
- 91 R. Moreddu, J. S. Wolffsohn, D. Vigolo and A. K. Yetisen, *Sens. Actuators, B*, 2020, **317**, 128183.
- 92 S. Yin, X. Chen, R. Li, L. Sun, C. Yao and Z. Li, *ACS Nano*, 2024, **18**, 18522–18533.

- 93 W. Ibrahim, M. J. Wilde, R. L. Cordell, M. Richardson, D. Salman, R. C. Free, B. Zhao, A. Singapuri, B. Hargadon, E. A. Gaillard, T. Suzuki, L. L. Ng, T. Coats, P. Thomas, P. S. Monks, C. E. Brightling, N. J. Greening, S. Siddiqui, R. Munton, J. Le Quesne, A. H. Goodall, H. C. Pandya, J. C. Reynolds, M. R. J. Clokie, N. J. Samani, M. R. Barer and J. A. Shaw, *Sci. Transl. Med.*, 2022, **14**, eabl5849.
- 94 R. A. Dweik, P. B. Boggs, S. C. Erzurum, C. G. Irvin, M. W. Leigh, J. O. Lundberg, A.-C. Olin, A. L. Plummer and D. R. Taylor, *Ann. Am. Thorac. Soc.*, 2011, **184**, 602–615.
- 95 P. Q. Nguyen, L. R. Soenksen, N. M. Donghia, N. M. Angenent-Mari, H. de Puig, A. Huang, R. Lee, S. Slomovic, T. Galbersanini, G. Lansberry, H. M. Sallum, E. M. Zhao, J. B. Niemi and J. J. Collins, *Nat. Biotechnol.*, 2021, **39**, 1366–1374.
- 96 C. M. Williams, A. K. Muhammad, B. Sambou, A. Bojang, A. Jobe, G. K. Daffeh, O. Owolabi, D. Pan, M. Pareek, M. R. Barer, J. S. Sutherland and P. Haldar, *Clin. Infect. Dis.*, 2023, **76**, e957–e964.
- 97 H. Yin and S. Mo, *Ann. Med.*, 2022, **54**, 1732–1737.
- 98 D. J. Kearney, T. Hubbard and D. Putnam, *Dig. Dis. Sci.*, 2002, **47**, 2523–2530.
- 99 G. Peng, U. Tisch, O. Adams, M. Hakim, N. Shehada, Y. Y. Broza, S. Billan, R. Abdah-Bortnyak, A. Kuten and H. Haick, *Nat. Nanotechnol.*, 2009, **4**, 669–673.
- 100 H. Li, H. Gong, T. H. Wong, J. Zhou, Y. Wang, L. Lin, Y. Dou, H. Jia, X. Huang, Z. Gao, R. Shi, Y. Huang, Z. Chen, W. Park, J. Y. Li, H. Chu, S. Jia, H. Wu, M. Wu, Y. Liu, D. Li, J. Li, G. Xu, T. Chang, B. Zhang, Y. Gao, J. Su, H. Bai, J. Hu, C. K. Yiu, C. Xu, W. Hu, J. Huang, L. Chang and X. Yu, *Nat. Commun.*, 2023, **14**, 7539.
- 101 W. Heng, S. Yin, J. Min, C. Wang, H. Han, E. Shirzaei Sani, J. Li, Y. Song, H. B. Rossiter and W. Gao, *Science*, 2024, **385**, 954–961.
- 102 M.-R. Chao, Y.-M. Shih, Y.-W. Hsu, H.-H. Liu, Y.-J. Chang, B.-H. Lin and C.-W. Hu, *Free Radical Biol. Med.*, 2016, **93**, 77–83.
- 103 J. Sun, K. Cheng and Y. Xie, *Biomolecules*, 2024, **14**, 1540.
- 104 S. Valdimarsson, U. Jodal, L. Barregård and S. Hansson, *Pediatr. Nephrol.*, 2017, **32**, 2079–2087.
- 105 S. Waldecker-Gall, C. B. Waldecker, N. Babel, X. Baraliakos, F. Seibert and T. H. Westhoff, *Sci. Rep.*, 2024, **14**, 12230.
- 106 S. Heytens, A. De Sutter, L. Coorevits, P. Cools, J. Boelens, L. Van Simaey, T. Christiaens, M. Vanechoutte and G. Claeys, *Clin. Microbiol. Infect.*, 2017, **23**, 647–652.
- 107 T. Bermudez, J. E. Schmitz, M. Boswell and R. Humphries, *J. Clin. Microbiol.*, 2025, **63**, e0030624.
- 108 S.-I. T. Palat, L. Biehle and L. Adler, *J. Am. Med. Dir. Assoc.*, 2024, **25**, 105031.
- 109 A. R. Levine, M. Tran, J. Shepherd and E. Naut, *Am. J. Emerg. Med.*, 2018, **36**, 1993–1997.
- 110 R.-Y. Xu, H.-W. Liu, J.-L. Liu and J.-H. Dong, *BMC Urol.*, 2014, **14**, 45.
- 111 W. Seo, W. Yu, T. Tan, B. Ziaie and B. Jung, *IEEE Trans. Biomed. Circuits Syst.*, 2017, **11**, 681–691.
- 112 W. Xu, M. Althumayri, A. Y. Tarman and H. Ceylan Koydemir, *Biosens. Bioelectron.*, 2025, **283**, 117539.
- 113 A. Childs, B. Mayol, J. A. Lasalde-Ramirez, Y. Song, J. R. Sempionatto and W. Gao, *ACS Nano*, 2024, **18**, 24605–24616.
- 114 S. Wan, Y. Wang, X. Li, J. Qiu, J. Liu and B. Gao, *Anal. Chem.*, 2025, **97**, 12467–12479.
- 115 P. Pandit, B. Crewther, C. Cook, C. Punyadeera and A. K. Pandey, *Mater. Adv.*, 2024, **5**, 5339–5350.
- 116 X. Liu, H. Yuk, S. Lin, G. A. Parada, T. C. Tang, E. Tham, C. de la Fuente-Nunez, T. K. Lu and X. Zhao, *Adv. Mater.*, 2018, **30**, 1870021.
- 117 M. E. Allen, E. Kamilova, C. Monck, F. Ceroni, Y. Hu, A. K. Yetisen and Y. Elani, *Adv. Sci.*, 2024, **11**, e2309509.
- 118 J. García-Alonso, G. M. Greenway, J. D. Hardege and S. J. Haswell, *Biosens. Bioelectron.*, 2009, **24**, 1508–1511.
- 119 M. Mirzaei, M. Pla-Roca, R. Safavieh, E. Nazarova, M. Safavieh, H. Li, J. Vogel and D. Juncker, *Lab Chip*, 2010, **10**, 2449–2457.
- 120 M. Mimee, P. Nadeau, A. Hayward, S. Carim, S. Flanagan, L. Jerger, J. Collins, S. McDonnell, R. Swartwout, R. J. Citorik, V. Bulovic, R. Langer, G. Traverso, A. P. Chandrakasan and T. K. Lu, *Science*, 2018, **360**, 915–918.
- 121 M. E. Inda-Webb, M. Jimenez, Q. Liu, N. V. Phan, J. Ahn, C. Steiger, A. Wentworth, A. Riaz, T. Zirtiloglu, K. Wong, K. Ishida, N. Fabian, J. Jenkins, J. Kuosmanen, W. Madani, R. McNally, Y. Lai, A. Hayward, M. Mimee, P. Nadeau, A. P. Chandrakasan, G. Traverso, R. T. Yazicigil and T. K. Lu, *Nature*, 2023, **620**, 386–392.
- 122 Q. Liu, M. Jimenez, M. E. Inda, A. Riaz, T. Zirtiloglu, A. P. Chandrakasan, T. K. Lu, G. Traverso, P. Nadeau and R. T. Yazicigil, *IEEE J. Solid-State Circuits*, 2023, **58**, 838–851.
- 123 P. Q. Nguyen, L. R. Soenksen, N. M. Donghia, N. M. Angenent-Mari, H. de Puig, A. Huang, R. Lee, S. Slomovic, T. Galbersanini, G. Lansberry, H. M. Sallum, E. M. Zhao, J. B. Niemi and J. J. Collins, *Nat. Biotechnol.*, 2021, **39**, 1366–1374.
- 124 I. Tanniche and B. Behkam, *J. Biol. Eng.*, 2023, **17**, 65.
- 125 L. Yang, Y. Gao, Q. Liu, W. Li, Z. Li, D. Zhang, R. Xie, Y. Zheng, H. Chen and X. Zeng, *Small*, 2024, **20**, e2307104.
- 126 D. He, X. Liu, J. Jia, B. Peng, N. Xu, Q. Zhang, S. Wang, L. Li, M. Liu, Y. Huang, X. Zhang, Y. Yu and G. Luo, *Adv. Funct. Mater.*, 2023, **34**, 2306357.
- 127 X. Zhang, M. M. Hasani-Sadrabadi, J. Zarubova, E. Dashtimighadam, R. Haghniaz, A. Khademhosseini, M. J. Butte, A. Moshaverinia, T. Aghaloo and S. Li, *Matter*, 2022, **5**, 666–682.
- 128 A. K. Nguyen, K. H. Yang, K. Bryant, J. Li, A. C. Joice, K. A. Werbovetz and R. J. Narayan, *Biomed. Microdevices*, 2019, **21**, 8.
- 129 Y. Xiang, J. Lu, C. Mao, Y. Zhu, C. Wang, J. Wu, X. Liu, S. Wu, K. Y. H. Kwan, K. M. C. Cheung and K. W. K. Yeung, *Sci. Adv.*, 2023, **9**, eadf0854.
- 130 A. M. Downs, A. Bolotsky, B. M. Weaver, H. Bennett, N. Wolff, R. Polsky and P. R. Miller, *Biosens. Bioelectron.*, 2023, **236**, 115408.

- 131 J. Zhou, D. Yao, Z. Qian, S. Hou, L. Li, A. T. A. Jenkins and Y. Fan, *Biomaterials*, 2018, **161**, 11–23.
- 132 Z. Pazhouhnia, A. Farzin, H. Rastgar, M. Dadgarnezhad and B. Jannat, *J. Biomed. Mater. Res., Part B*, 2024, **112**, e35454.
- 133 Y. Jiang, A. A. Trotsyuk, S. Niu, D. Henn, K. Chen, C.-C. Shih, M. R. Larson, A. M. Mermin-Bunnell, S. Mittal, J.-C. Lai, A. Saberli, E. Beard, S. Jing, D. Zhong, S. R. Steele, K. Sun, T. Jain, E. Zhao, C. R. Neimeth, W. G. Viana, J. Tang, D. Sivaraj, J. Padmanabhan, M. Rodrigues, D. P. Perrault, A. Chattopadhyay, Z. N. Maan, M. C. Leeolou, C. A. Bonham, S. H. Kwon, H. C. Kussie, K. S. Fischer, G. Gurusankar, K. Liang, K. Zhang, R. Nag, M. P. Snyder, M. Januszyk, G. C. Gurtner and Z. Bao, *Nat. Biotechnol.*, 2023, **41**, 652–662.
- 134 Q. Huang, F. He, J. Yu, J. Zhang, X. Du, Q. Li, G. Wang, Z. Yu and S. Chen, *J. Mater. Chem. B*, 2021, **9**, 2727–2735.
- 135 A. Than, C. Liu, H. Chang, P. K. Duong, C. M. G. Cheung, C. Xu, X. Wang and P. Chen, *Nat. Commun.*, 2018, **9**, 4433.
- 136 M. Cui, M. Zheng, C. Wiraja, S. W. T. Chew, A. Mishra, V. Mayandi, R. Lakshminarayanan and C. Xu, *Adv. Sci.*, 2021, **8**, e2102327.
- 137 S. Sillankorva, L. Pires, L. M. Pastrana and M. Banobre-Lopez, *Viruses*, 2022, **14**, 964.
- 138 S. Ray, D. M. Wirth, O. A. Ortega-Rivera, N. F. Steinmetz and J. K. Pokorski, *Biomacromolecules*, 2022, **23**, 903–912.
- 139 A. Donadei, H. Kraan, O. Ophorst, O. Flynn, C. O'Mahony, P. C. Soema and A. C. Moore, *J. Controlled Release*, 2019, **311–312**, 96–103.
- 140 V. T. T. Nguyen, N. Darville and A. Vermeulen, *AAPS J.*, 2022, **25**, 4.
- 141 S. Yu, H. Sun, Y. Li, S. Wei, J. Xu and J. Liu, *Mater. Today Bio*, 2022, **16**, 100435.
- 142 X. Zhou, J. Zhang, X.-M. Deng, F.-M. Fu, J.-M. Wang, Z.-Y. Zhang, X.-Q. Zhang, Y.-X. Luo and S.-Y. Zhang, *Sci. Rep.*, 2024, **14**, 22673.
- 143 C. Wang, K. Fan, E. Shirzaei Sani, J. A. Lasalde-Ramirez, W. Heng, J. Min, S. A. Solomon, M. Wang, J. Li, H. Han, G. Kim, S. Shin, A. Seder, C. D. Shih, D. G. Armstrong and W. Gao, *Sci. Transl. Med.*, 2025, **17**, eadt0882.
- 144 Y. Song, R. Y. Tay, J. Li, C. Xu, J. Min, E. Shirzaei Sani, G. Kim, W. Heng, I. Kim and W. Gao, *Sci. Adv.*, 2023, **9**, eadi6492.
- 145 J. Jeon, S. Lee, S. Chae, J. H. Lee, H. Kim, E. S. Yu, H. Na, T. Kang, H. S. Park, D. Lee and K. H. Jeong, *Nat. Commun.*, 2025, **16**, 8017.
- 146 X. Li, S. Wan, T. S. Pronay, X. Yang, B. Gao and C. T. Lim, *Nanoscale Horiz.*, 2025, **10**, 1815–1837.
- 147 S. M. Shafi and S. K. Chinnappan, *PeerJ Comput. Sci.*, 2024, **10**, e2444.
- 148 N. Vyas, A. Sharma, A. Nayyar, M. Shrivastava and D. Gowda, *Proceedings of the International Conference on Advancements in Computing Technologies and Artificial Intelligence (COMPUTATIA 2025)*, Atlantis Press International BV, 2025.
- 149 F. S. Bashiri, K. A. Carey, J. Martin, J. L. Koyner, D. P. Edelson, E. R. Gilbert, A. Mayampurath, M. Afshar and M. M. Churpek, *JAMIA Open*, 2024, **31**, 1322–1330.
- 150 P. Madan, V. Singh, V. Chaudhari, Y. Albagory, A. Dumka, R. Singh, A. Gehlot, M. Rashid, S. S. Alshamrani and A. S. AlGhamdi, *Appl. Sci.*, 2022, **12**, 3989.
- 151 M. A. Zahed, D. K. Kim, S. H. Jeong, M. Selim Reza, M. Sharifuzzaman, G. B. Pradhan, H. Song, M. Asaduzzaman and J. Y. Park, *ACS Sens.*, 2023, **8**, 2960–2974.
- 152 S. Fortunati, C. Giliberti, M. Giannetto, A. Bolchi, D. Ferrari, G. Donofrio, V. Bianchi, A. Boni, I. De Munari and M. Careri, *Biosensors*, 2022, **12**, 426.
- 153 Anjali, H.-N. Dai, J. Kumar and O. J. Pandey, *IEEE Sens. J.*, 2023, **23**, 29804–29814.
- 154 C. Szydzik, A. F. Gavela, J. Roccisano, S. Herranz de Andrés, A. Mitchell and L. Lechuga, *Towards an integrated optofluidic system for highly sensitive detection of antibiotics in seawater incorporating bimodal waveguide photonic biosensors and complex, active microfluidics*, SPIE, 2016.
- 155 Y. Liu, L. Yang and Y. Cui, *Microsyst. Nanoeng.*, 2024, **10**, 112.
- 156 J. Yu, Y. Zhang, Y. Ye, R. DiSanto, W. Sun, D. Ranson, F. S. Ligler, J. B. Buse and Z. Gu, *Proc. Natl. Acad. Sci. U. S. A.*, 2015, **112**, 8260–8265.
- 157 Y. Abdelaal, M. Aupetit, A. Baggag and D. Al-Thani, *J. Med. Internet Res.*, 2024, **26**, e53863.
- 158 K. Naruse, *Biophys. Rev.*, 2018, **10**, 1257–1262.
- 159 A. Persat, C. D. Nadell, M. K. Kim, F. Ingremeau, A. Siryaporn, K. Drescher, N. S. Wingreen, B. L. Bassler, Z. Gitai and H. A. Stone, *Cell*, 2015, **161**, 988–997.
- 160 Y. Zhou, X. Zhou, X. Zhu, F. Xu and F. Li, *Cell Rep. Phys. Sci.*, 2025, **6**, 102612.
- 161 A. Brugues, E. Anon, V. Conte, J. H. Veldhuis, M. Gupta, J. Colombelli, J. J. Munoz, G. W. Brodland, B. Ladoux and X. Trepast, *Nat. Phys.*, 2014, **10**, 683–690.
- 162 Y. Zhou, X. Zhou, J. Zhang, Y. Zhao, Z. Ye, F. Xu and F. Li, *Anal. Chem.*, 2025, **97**, 5517–5526.
- 163 J. Nijjer, C. Li, M. Kothari, T. Henzel, Q. Zhang, J.-S. B. Tai, S. Zhou, T. Cohen, S. Zhang and J. Yan, *Nat. Phys.*, 2023, **19**, 1936–1944.
- 164 J. E. Sanfilippo, A. Lorestani, M. D. Koch, B. P. Bratton, A. Siryaporn, H. A. Stone and Z. Gitai, *Nat. Microbiol.*, 2019, **4**, 1274–1281.
- 165 V. Tokárová, A. Sudalaiyadum Perumal, M. Nayak, H. Shum, O. Kašpar, K. Rajendran, M. Mohammadi, C. Tremblay, E. A. Gaffney, S. Martel, D. V. Nicolau and D. V. Nicolau, *Proc. Natl. Acad. Sci. U. S. A.*, 2021, **118**, e2013925118.
- 166 E. E. Bastounis, P. Radhakrishnan, C. K. Prinz and J. A. Theriot, *Microbiol. Mol. Biol. Rev.*, 2022, **86**, e0009420.
- 167 H. J. Kim, D. Huh, G. Hamilton and D. E. Ingber, *Lab Chip*, 2012, **12**, 2165–2174.
- 168 M. Ballerini, S. Galiè, P. Tyagi, C. Catozzi, H. Raji, A. Nabinejad, A. D. G. Macandog, A. Cordiale, B. I. Slivinski, K. K. Kugiejko, M. Freisa, P. Occhetta, J. A. Wargo, P. F. Ferrucci, E. Cocorocchio, N. Segata, A. Vignati, A. Morgun, M. Deleidi, T. Manzo, M. Rasponi and L. Nezi, *Nat. Biomed. Eng.*, 2025, **9**, 967–984.
- 169 R. Chawla, R. Gupta, T. P. Lele and P. P. Lele, *J. Mol. Biol.*, 2020, **432**, 523–533.

- 170 G. Yao, X. Mo, C. Yin, W. Lou, Q. Wang, S. Huang, L. Mao, S. Chen, K. Zhao, T. Pan, L. Huang and Y. Lin, *Sci. Adv.*, 2022, **8**, eabl8379.
- 171 L. Chang, H. Du, F. Xu, C. Xu and H. Liu, *Trends Biotechnol.*, 2024, **42**, 31–42.
- 172 Z. Du, G. Zhao, A. Wang, W. Sun and S. Mi, *ACS Appl. Polym. Mater.*, 2022, **4**, 7290–7299.
- 173 N. Xie, J. Tian, Z. Li, N. Shi, B. Li, B. Cheng, Y. Li, M. Li and F. Xu, *Phys. Life Rev.*, 2024, **51**, 328–342.
- 174 G. Bart, D. Fischer, A. Samoylenko, A. Zhyvolozhnyi, P. Stehantsev, I. Miinalainen, M. Kaakinen, T. Nurmi, P. Singh, S. Kosamo, L. Rannaste, S. Viitala, J. Hiltunen and S. J. Vainio, *BMC Genomics*, 2021, **22**, 425.
- 175 E. C. Townsend and L. R. Kalan, *Biochem. Soc. Trans.*, 2023, **51**, 71–86.
- 176 F. Bakhshandeh, H. Zheng, N. G. Barra, S. Sadeghzadeh, I. Ausri, P. Sen, F. Keyvani, F. Rahman, J. Quadrilatero, J. Liu, J. D. Schertzer, L. Soleymani and M. Poudineh, *Adv. Mater.*, 2024, **36**, 2313743.
- 177 V. Thammavongsa, D. M. Missiakas and O. Schneewind, *Science*, 2013, **342**, 863–866.
- 178 Y. Liao, Z. Zhang, Y. Zhao, S. Zhang, K. Zha, L. Ouyang, W. Hu, W. Zhou, Y. Sun and G. Liu, *Bioact. Mater.*, 2025, **44**, 131–151.
- 179 O. Simoska, J. Duay and K. J. Stevenson, *ACS Sens.*, 2020, **5**, 3547–3557.
- 180 K. Wu, X. Wu, M. Chen, H. Wu, Y. Jiao and C. Zhou, *Chem. Eng. J.*, 2020, **387**, 124127.
- 181 B. Rai, S. Kharb, R. Jain and S. C. Anand, *J. Oral Sci.*, 2008, **50**, 53–56.
- 182 DOI: [10.1016/B978-1-4377-1984-0.00024-3](https://doi.org/10.1016/B978-1-4377-1984-0.00024-3).
- 183 E. Y. H. Xin, G. Kwek, X. An, C. Sun, S. Liu, N. S. Qing, S. Lingsh, L. Jiang, G. Liu and B. Xing, *Angew. Chem.*, 2024, **63**, e202406843.